Master's Thesis

Development and Implementation of a Wireless Sensor Network including Positioning for optimizing Cattle Breeding

Manuel Frech

Institute for Electronics

Graz Universtiy of Technology

Head: Univ.-Prof. Dipl.-Ing. Dr.techn. Wolfgang Pribyl

Assessor: Ass.Prof. Dipl.-Ing. Dr.techn. Gunter Winkler

Advisor: Dipl.-Ing. Dr.techn. Stefan Rosenkranz

Graz, November 2011

Abstract

Over the last years technological progress has also caused changes in animal husbandry. Nowadays *Precision Livestock Farming* systems support farmers during their daily work and in cattle breeding with the use of electronic devices.

In this thesis an electronic system has been developed that supports stockmen in cattle breeding. It is used for the detection of peak estrus and parturition, two critical parts in the life cycle of cows, that can lead to avoid financial losses. With the help of this system heat can be detected automatically, so the optimal time for insemination can be found, and the farmer can be informed about an upcoming calving event to avoid injuries at dam and calf.

Keywords: heat detection, calving detection, sensor system, veterinary telematics, Precision Livestock Farming

Kurzfassung

In den letzten Jahren hat der technische Fortschritt auch Viehwirtschaft erreicht. Unter dem Sammelbegriff *Precision Livestock Farming* helfen heutzutage eine Vielzahl elektronischer Geräte dem Landwirt beim Erledigen seiner täglichen Arbeiten und bei der Überwachung seiner Rinder.

In dieser Diplomarbeit ist ein elektronisches System entwickelt worden, das den Landwirt bei der Aufzucht der Rinder unterstützt. Es dient zur Brunst- und Geburtendetektion, zwei kritische Zeitpunkte im Lebenszyklus von Rindern, die zu Profiteinbußen führen können. Mit Hilfe dieses Systems soll einerseits die Brunst automatisch erkannt werden, um eine Befruchtung zum optimalen Zeitpunkt vornehmen zu können, und andererseits der Bauer über eine bevorstehende Geburt rechtzeitig informiert werden, um Verletzungen an Kuh und Kalb vermeiden zu können.

Schlüsselwörter: Brunsterkennung, Geburtendetektion, Sensorsystem, Veterinärtelematik, Precision Livestock Farming

STATUTORY DECLARATION

I declare that I have authored this thesis independently, that I have not used other than the declared sources / resources, and that I have explicitly marked all material which has been quoted either literally or by content from the used sources.

....
date (signature)

EIDESSTATTLICHE ERKLÄRUNG

Ich erkläre an Eides statt, dass ich die vorliegende Arbeit selbstständig verfasst, andere als die angegebenen Quellen/Hilfsmittel nicht benutzt und die den benutzten Quellen wörtlich und inhaltlich entnommene Stellen als solche kenntlich gemacht habe.

Graz, am ....
(Unterschrift)

Acknowledgement

This master's thesis was accomplished at the Institute for Electronics at Graz University of Technology in the year 2011.

At first I want to thank Dr. Stefan Rosenkranz and Mario Fallast, who enabled the establishment of my master's thesis at their company smaXtec product development GmbH and supported me during my work.

Special thanks are due to my mentor and assessor Dr. Gunter Winkler for his support in my master studies and his never ending effort in teaching.

Finally, I want to thank my parents for their support during my whole educational and academic training over the past years.

Tank you all.

Graz, November 2011 Manuel Frech

Contents

List of Figures

List of Tables

1 Introduction

The type of livestock farming has changed over the last 40 years from self-sustaining farms holding a small amount of different animals to farms, where a single species (or animal source food) is mass-produced. A stockman has always been responsible for all aspects of animal husbandry and he usually wants to achieve high profit, leading to the need of ideal conditions for animal growth and production. Nowadays livestock production is no longer limited to fulfill economic targets, as consumer requirements concerning food safety and quality have to be met and these requirements become increasingly well defined. Furthermore, efficient and sustainable animal farming, healthy animals, guaranteed animal well being and acceptable environmental impact of livestock production concerns todays society as well [1, 2].

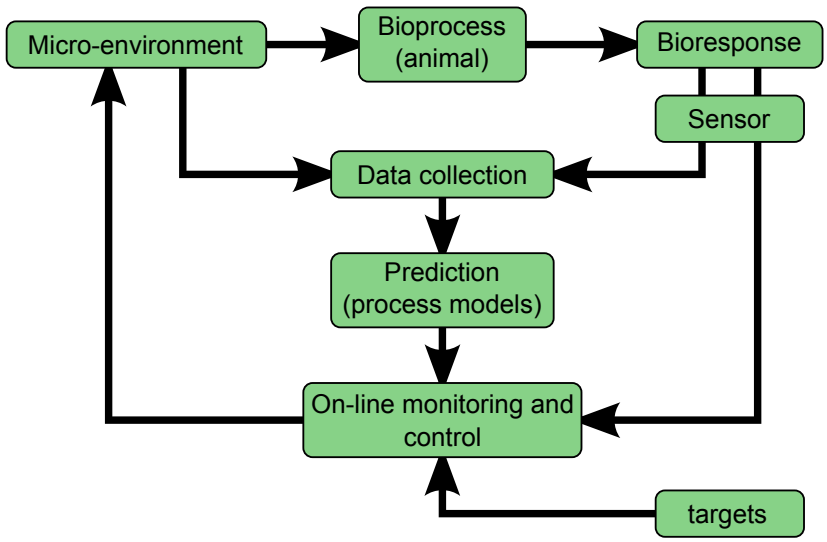

Figure 1.1: A schematic overview of *Precision Livestock Farming* (PLF) with sensors measuring the biological response of animals, various processing models for data analyzing and a monitoring and control system [2]

Increasing herd and farm size and higher customer standards have led to the development of monitoring system techniques, that assist stockmen at their work. *Precision Livestock Farming* systems (see figure 1.1) gather and store data of various sensors in databases, evaluate all data by mathematical process models and feed the outcome into an on-line monitoring and a controlling system, that allows (or even performs) changing in the environment of animals (feeding, climate, etc). The combination of different sensor data (done in the mathematical process models) allows an interpretation of animal condition and counteractions to be taken. Therefore, the use of PLF can improve efficiency in production, enable an easy way of quality

control and provide products to customers with a given specification and known production history [1, 2].

Kwong et al. [3] have perfectly summarized the benefits of PLF:

> *"By monitoring and understanding cattle's individual and herd behavior, farmers can potentially identify the onset of illness, lameness or other conditions which might benefit from early intervention.*
>
> *Low cost sensor network platforms show considerable potential in this context but are faced with a number of significant technical challenges before they are widely and routinely adopted."* (Kwong et al., 2008 [3])

This thesis deals with problems during the animal life cycle, especially the reproduction cycle. The process of parturition can implicate severe problems, where dam and calf can suffer injuries or even die in the worst case, if obstetrical assistance is not applied in time [4, 5]. Also fertilizations has been identified as a major problem in cattle, because cows are inseminated at the wrong time due to faulty heat detection [6]. These facts lead to financial losses for farms, that can be avoided by electronic aids what would result in an increased production efficiency. The newly developed system addresses the two problems of calving and heat detection and is intended to expand the PLF system of smaXtec.

1.1 Veterinary Background and Economic Considerations

Some basic knowledge on parturition and estrous cycle will be given in the following subsections concerning not only veterinary, but also economic aspects. The content is based on research done in the last 60 years and published in [7, 5, 4, 8, 9].

1.1.1 Reproduction Cycle in Cattle

According to J.A. Parish et al. [10], the female reproduction cycle in cattle can be divided into six stages:

1. **Prepubertal:** Growing heifers do not exhibit an estrous cycle (*anestrous*).
2. **Puberty:** Puberty begins with the first estrus. At the age of about eleven months calves typically enter the stage of puberty. The age at puberty depends on genetics (breeds differ in onset of puberty) and weight (lower weight gains can decelerate puberty).
3. **Estrous Cycles:** Cattle show continues estrous cycles with even intervals of typical 21 days (±3 days). In this stage fertilization must be done during standing heat lasting for typical 15 hours (±9 hours).
4. **Gestation:** After a successful fertilization, a cow is gestating for approximately 281 days (±11 days). During pregnancy cows are non-cycling. The length of gestations depends on the number, breed and sex of fetuses [8].

5. **Parturition:** Calving can occur within a few hours or as long as a day after the gestating cow becomes restless [8]. Other studies show that chemical and physical changes occur up to 48 hours before parturition [7, 9].

6. **Postpartum:** The period of recovery after calving lasts for typically ≥ 40 days and during that time cattle are again *anestrous*, as they do not show signs of heat. After this stage, the estrous cycle begins again.

Estrous Cycles and *Parturition* can be seen as two critical stages concerning breeding efficiency. During the estrous cycle the correct timing for insemination must be found to shorten the time between parturition and gestation (stage six *Postpartum*). At parturition often obstetrical assistance is needed to avoid injuries and to assure survival of dam and calf. Shorter calving intervals and each survived animal result in more calves over a cow's lifetime, and therefore increase milk production (in dairy cattle) and meat production (in beef cattle).

1.1.2 Estrous Cycle and Heat Detection

The estrous cycle of cattle with a typical interval of 21 days can be divided into the following four phases [11, 12] and is illustrated in figure 1.2:

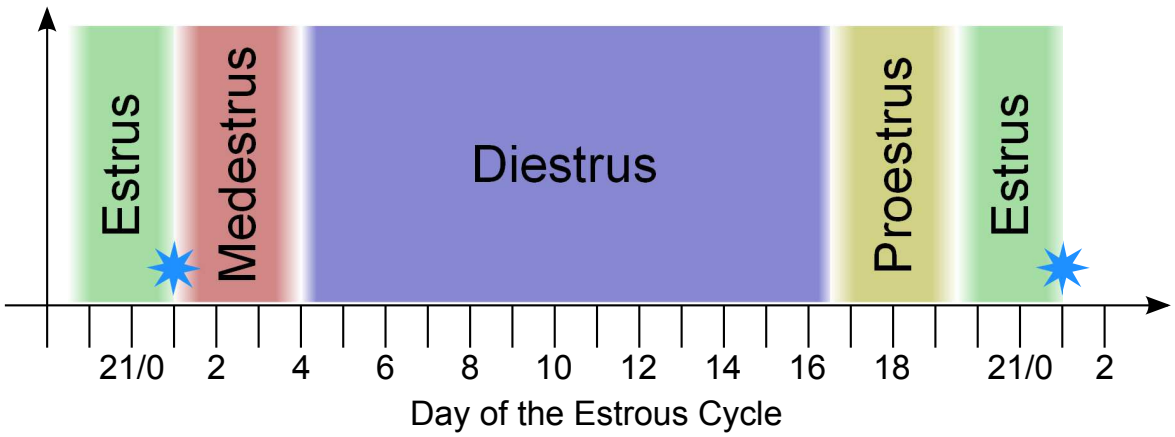

Figure 1.2: The four phases of an estrous cycle of cattle. The blue stars mark the ovulation and the start of the cycle.

proestrus: Change in animal behavior (smells other cows, headbutts other cows, attempts to ride other cows) lasting for two to three days before estrus indicate an upcoming onset of a new estrous cycle. This phase occurs before the current estrous cycle starts, so it actually belongs to the previous one.

estrus: For 28 to 36 hours cows or heifers are in estrus. During a time window of nine to 18 hours, they exhibit signs of estrus like riding other cows and standing to be mounted. Ovulation occurs at the end of *estrus*, stated as day 1 of the cycle.

metestrus: After the ovulation the animal enters the two to three days lasting *metestrus* (or *postestrus*), where heat symptoms decline and disappear. Also bloody mucus often appears around the vulva during that phase.

diestrus: The rest of the estrous cycle the cow is sexually non for about 16 days.

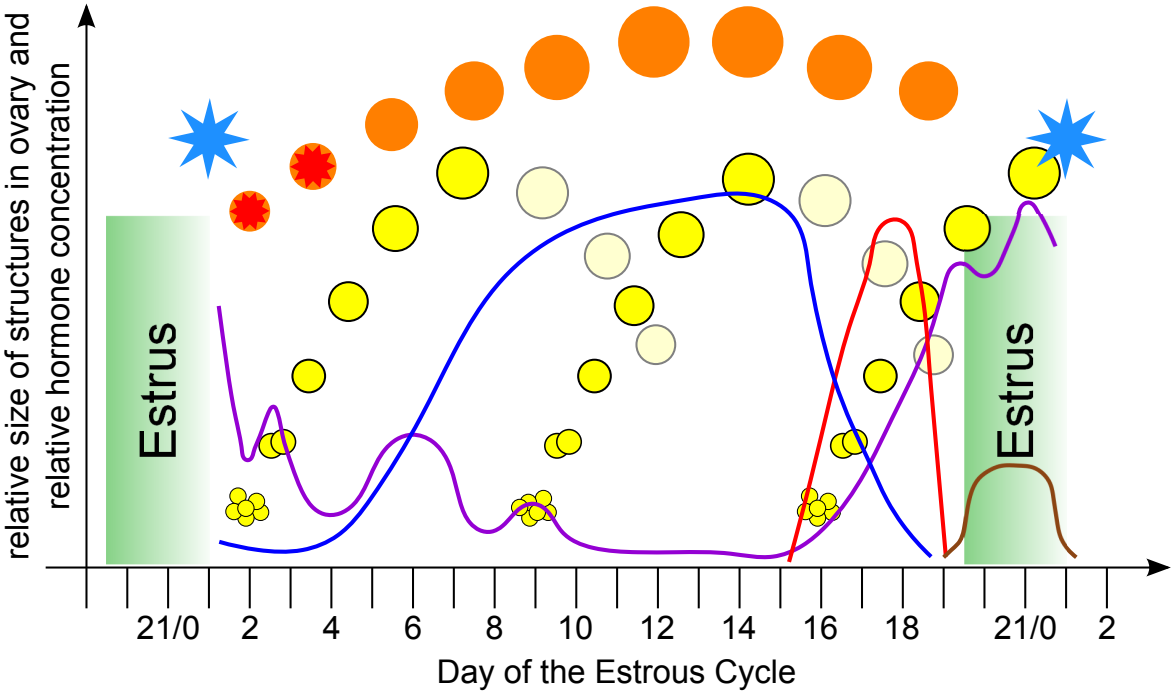

Figure 1.3: Illustration of the estrous cycle of cattle showing the phase of estrus (green), two ovulations (blue stars), corpus luteum (red & orange circles), progesterone level (blue), prostaglandin $F_{2\alpha}$ level (red), follicles (yellow circles), luteinizing hormone level (brown), estrogen level (violet)

Figure 1.3 illustrates the estrous cycle in cattle with hormonal changes and growing structures in the ovary. The tissue of the ruptured follicle (red stars in orange circles) turns into the corpus luteum (referred to as CL and visualized with orange circles) around day five of the cycle and produces progesterone (blue), a hormone needed to establish and maintain pregnancy. The progesterone-dominant luteal phase (matches the *diestrus* phase) spans from day five to 17 and is a period of sexual rest [10, 12, 13].

Around day 17 the CL will be lysed, if no pregnancy has resulted from the previous ovulation. This is done by the uterus, that produces the hormone prostaglandin $F_{2\alpha}$ (further referred to as $PGF_{2\alpha}$ and colored in red), that causes the regression of CL in the following three to five days. If the animal has successfully been fertilized and is pregnant, the release of $PGF_{2\alpha}$ from the uterus is prevented by the embryo and the CL keeps on producing progesterone. At this point, the animal gets into the *proestrus* phase again [10, 12, 13].

The growth of follicles (yellow circles) in the ovary is controlled by the follicle stimulating hormone (FSH) and the luteinizing hormone (LH), which are produced by the pituitary

gland. When FSH is released, a group of follicles starts to grow, but only one follicle of the group remains and matures whereas the others die off and regress. When the animal is not pregnant and is at the end of the estrous cycle (when the CL has been lysed), the progesterone concentration in the blood is very low. This allows LH to reach higher level, what finally causes the ovulation to occur. This surge in LH (brown) is triggered by the hormone estrogen (violet) produced in the follicle, what also changes cow's behavior and make them conceptive. If progesterone concentration in the blood is still high (during luteal phase or in pregnancy), the matured follicle regresses as well and a new group starts growing. Two to three follicle groups (follicle waves) are usually being recruited during an estrous cycle [10, 12].

The oocyte can be fertilized within six to 24 hours after ovulation [13], and therefore the time of ovulation somehow has to be detected. As prior mentioned, cycling cows change their behavior in *proestrus* and *estrus* phase and show different signs of heat.

> *"Visual observation is a commonly used method of heat detection. It involves a trained observer's recognizing and recording signs of heat. Observable signs of heat include mounting or attempting to mount other cattle, standing to be mounted by other cattle, smelling other females, trailing other females, bellowing, depressed appetite, nervous and excitable behavior, mud on hindquarters and sides of cattle, roughed up tail hair, vulva swelling and reddening, clear vaginal mucous discharge, and mucous smeared on rump.*
>
> *The surest sign of heat is when a cow or heifer allows other cattle to mount her while she remains standing. This is called standing heat. Cattle may be willing to mount others but may not stand to be mounted when outside of standing heat. This usually indicates she is either coming into or going out of standing heat."* (Parish et al., 2010 [11])

Standing heat typically lasts for five to ten seconds, and therefore it is important to observe carefully [14]. Observation done by farmers or herdsmen should be done at least twice a day, for best results in the early morning and late in the evening for at least 30 minutes each. Cows should be observed away from feed-bunks and hayracks (hungry cattle might be more interested in the feed) and should be on a non-slippery ground with plenty of free moving space [11, 15]. More and longer observations increase efficiency of heat detection (see table 1.1) but keep labor from doing other works [14].

number of times observed for heat	**observed period**			
	10 minutes	**20 minutes**	**30 minutes**	**60 minutes**
1x daily	22%	31%	36%	39%
2x daily	33%	43%	55%	61%
3x daily	45%	55%	65%	71%
4x daily	49%	61%	71%	78%

Table 1.1: Efficiency of heat detection for different observation periods and quantity [14]

P.L. Senger has analyzed plenty of publications and stated, that heat detection efficiency is $\leq 50\%$ in most dairy herds and progesterone analysis have shown that up to 30% of all

inseminations are done out of estrus. Increasing herd size also leads to a decreasing heat detection rate due to lower manpower input per cow [6].

time of day	**percentage of cows showing heat signs**
6:00am - noon	22%
noon - 6:00pm	10%
6:00pm - midnight	25%
midnight - 6:00am	43%

Table 1.2: Percentage of cows showing heat signs at different times of the day (based on research by Cornell University)

A research done at Cornell University shows, that 68% of cows display heat signs outside duty hours (see table 1.2), so the majority of exhibited signs cannot be visually recognized by herdsmen. Therefore some aids for heat detection can be used [11, 14, 15]:

- **Chin-ball markers** mounted on oxen or cows treated with testosterone or "gomer" bulls. The marker paints the back or rump of a cow that is mounted. Analyzing the amount of paint on a cow leads to a detection of heat.
- **Tail Head Markers** are used at many U.S. dairies [15]. Chalk, crayon or paste is applied onto the tailhead of cows, that are expected to be in heat. If a cow is in standing heat, the paint gets rubbed off. Reading the chalk strip requires observation and some practice.
- **Pressure-sensitive pads** glued onto an animals tail can be used to find animals in heat. When prolonged pressure is applied, the pad changes its color. Animals that have been mounted more often and longer, will show a more significant color change.
- **Electronic aids** for heat detection are described in section 2.3.

Wrenn et al. [16] have found, that the body temperature also changes with the estrous cycle being lowest one to two days before estrus, high on the day of estrus and low again at the time of ovulation. Temperature change has further been analyzed and proofed in other researches [17, 18]

Also an increase in physical activity during estrus has been observed by video taping cattle and analyzing the videotape of each day concerning number of mounts, feeding, drinking, resting and walking activities (Hurnik et al. [19]). They have also confirmed that cows show more mounting activity during nocturnal period (as already stated in table 1.2). The increased activity has later been confirmed using pedometer measurements by C.A. Kiddy [20].

A more accurate detection of heat combined with artificial insemination can increase reproduction rate and therefore increase profitability [21]. The financial losses due to missed heat in the UK is estimated from £4 to £12 per missed heat (depending on time after calving) [22], and in the USA Senger estimated $300,000,000 per year for the whole dairy industry [6]. Van Vliet et al. have analyzed and summarized publications on results of breeding in

dairy cows of different countries in [23]. They give a total loss due to suboptimal fertility of $119,000,000 for The Netherlands, and state declining breeding results in other countries all over the world as well.

1.1.3 Parturition

The gravidity duration of cattle ranges from 270 to 292 days. At the end of gestation, parturition is initiated by the hypothalamo-pituitary axis of the fetus (see figure 1.4) producing the adrenocorticotropic hormone (ACTH), that causes growth of the fetal adrenal glands and leads to production of cortisol. Target of fetal cortisol is the placenta where it causes an increasing concentration of estrogen (E) in the dam. In response to E, the level of prostaglandin $F_{2\alpha}$ ($PGF_{2\alpha}$) rises, leading to an regression of the corpus luteum resulting in the termination of progesterone production, and receptors for oxytocin are developed. The elevated $PGF_{2\alpha}$ also causes release if oxytocin and prolactin (pituitary) and relaxin (ovarian). These maternal hormonal changes result in expansion of the birth canal, initiation of uterine contraction, maternal behavior, synthesis of milk and the ability to eject milk [8].

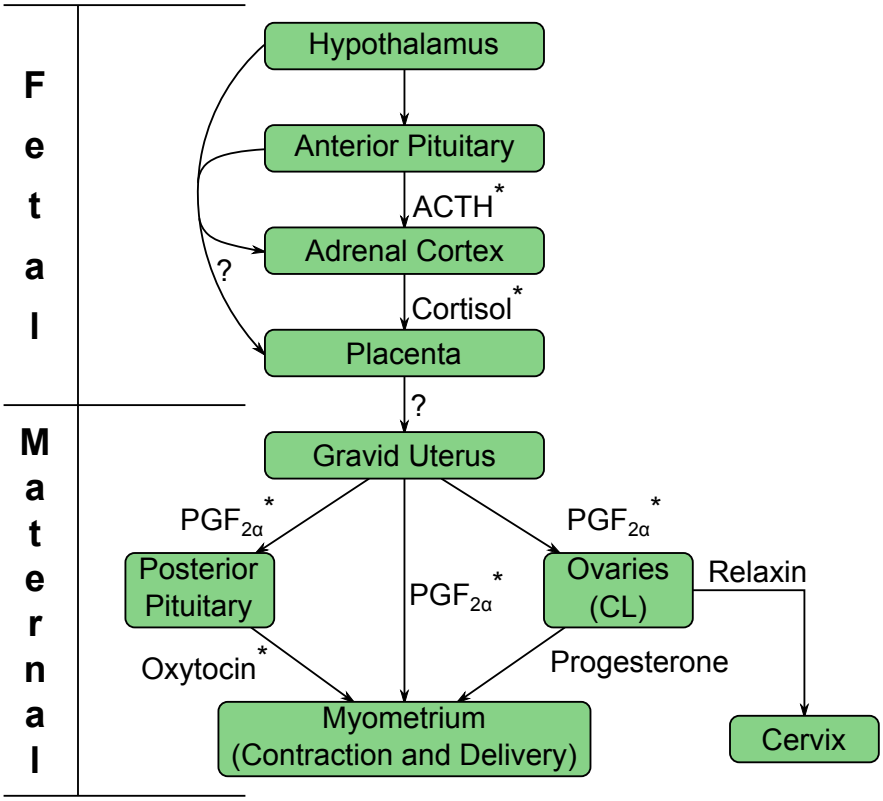

Figure 1.4: A suggested sequence of events leading to and associated with parturition in animals, where pregnancy is maintained by the ovaries (cattle). Hormones marked with an asterisk having a stimulatory effect on a target, **?** indicate unknown steps or compounds [8].

The body temperature seems to be closely related to the hormonal changes (esp. progesterone) in dam, resulting in temperature changes within 48 to 8 hours before parturition of up to 1°C [9]. Other external signs of impending parturition are: udder starting to fill out, swelling of vulva, and relaxation of pelvic ligaments. During the process of parturition, the following signs give information on the progress of calving (in order of appearance): restlessness, onset of labor, abdominal pressure, sighting of and rupture of allantochorion, rupture of amnion, first sight of calf's feet, and calf on the ground [5].

Aoki et al. compared two different approaches of detecting parturition by analyzing maternal temperature. In the "same hours method", temperature at a particular time of day has been compared to the same time of the preceding day. With temperature differences ≥ 0.3°C or ≥ 0.5°C for more than three hours, a calving has been detected. This method resulted in a detection rate of 100%. By comparing maximum and minimum values of temperature of a day to preceding days, a lower detection rate of 75% has been achieved [7].

Petterson et al. analyzed calvings over 15 years and figured out, that in the 6.7% death calves (893 out of 13,296 calvings) 68.8% died within 4 days after parturition because of dystocia [4], where about the half of these losses could be avoided by assisting at the birth. In another research by Berglund et al. over seven years with 159 cows (from first calving and their subsequent calvings) 30% of all parturitions (493, including seven stillbirths) needed slight assistance (manual pulling) at the end of parturition, and in 3% veterinary assistance has been given [5].

Every dead dam or calf comes with enormous financial loss. With a calving detection system, it would be easier and more convenient for a supervisor to monitor the process of parturition and intervene with obstetrical assistance or contact a veterinarian, if severe problems occur.

1.2 Outline

Chapter 2 discusses the main objectives of the thesis and describes different ways and possibilities of realizing both, calving and estrus detection. It also includes considerations and tests on the feasibility of three potential approaches.

The best approach has then been realized and a full hardware and firmware description over the whole system is given in **chapter 3**.

Evaluation of the developed solution and the integrated parts, that proofs the correct functionality, is shown in **chapter 4**. Several tests have been performed and the results are given and discussed.

Finally, Conclusion and Outlook (**chapter 5**) summarizes the thesis' content and describes the additional effort, that has to be made to successfully put calving and estrus detection into practice. It also gives some ideas of future projects and lists possible fields of application for the developed hardware.

2 Sensors and Solutions

smaXtec has already developed a radiotelemetric system to monitor temperature and pH value in the rumen of dairy cows. The measured data is sent to a smaXtec Base Station that is connected to the Internet. All data is stored in a central database where farmers have access to the measured values of cows in their farm.

2.1 System Integration

As part of this thesis the new developed system has to be integrated into smaXtec's radiotelemetric system. Therefore it is necessary to use a 433MHz transceiver and implement the protocol used for communication. Nevertheless the new sensors somehow have to be distinguished from the smaXtec pH Boluses, that the Base Station is able to interpret the read data correctly. The pH Bolus uses a MSP430 controller with an external CC1101 RF transceiver. The new system shall use the CC430 microcontroller that comes with a MSP CPU and an integrated RF core (see chapter 3).

2.2 Calving Detection

The course of parturition has been described in subsection 1.1.3. Electronic ways of detecting the onset of parturition are measuring body temperature and physical activity. Analyzing blood samples concerning the level of hormones, that can lead to a prediction of parturition, cannot be done inexpensively and continuously, and therefore has been neglected.

Temperature samples at the skin (with thermal infrared scanning of the gluteal region), of the milk (during milking) or in the rectum cannot be gathered automatically. The best way of continuously and accurately measuring body temperature is vaginal or ruminal [24, 25]. A surgical implantation of a temperature sensing device (like it has been used in [9]) has been agreed to be out of question. Physical activity can be measured with pedometers or activity meters [20].

With a vaginally inserted activity sensor in a dam, one can also determine the moment when the sensor has been expelled. This can be done by either detecting the freefall event, or measuring low motion [1].

[1] Author's note: This technique has not been found in publications, but seems to be a reasonable source for an urgent calving alarm.

Considering the details mentioned above leads to the development of a vaginal sensor device combining both, temperature and activity measurements.

2.3 Estrus Detection

The physical changes during the estrus cycle in cattle have been described in subsection 1.1.2. Some of these changes can be monitored by electronic and computer aided heat detection mechanisms, that have already been developed and tested [26]:

- **Heat Mount Detectors** record the mounting activity, concerning quantity and duration of mounts, using pressure sensor pads glued onto the rump of cattle, that are expected to be in heat.
- **Vaginal Conductivity** (or vaginal resistance) of the vaginal tissues and discharges can be measured to detect peak estrus.
- **Pedometers and Activity Meters** can detect increased physical activity, because cows in heat are more mobile.
- **Video Cameras** recording housed cattle can also be used. Videotapes can be analyzed afterwards looking for signs of estrus (standing heat).
- **Electronic Odor Detectors** analyzing the perineal odor can used to detect changes associated with heat.
- **Temperature Measurement** of skin, body (vaginal or ruminal) or milk have also been found to detect estrus in cattle [25].
- **Milk Progesterone Detection** directly analyzes the hormonal change throughout the estrous cycle. Cows can be fertilized on the third day of low progesterone level.
- **Tail Painting with Camera** measuring the paint removed of the cow's tail head can figure out cows, that have been more willing to be mounted (in standing heat).

A setup for calving detection combining vaginal temperature measurement and activity meter has already been chosen in section 2.2. Both, body temperature [16] and motion data [20] are also significant values for heat detection. Other values, that can be measured continuously, electrically and without the need of a human operator have not been found during the research. Therefore, calving and estrus detection can be combined into a single device, what leads to a lower price for customers and lower production costs (higher quantity of the same hardware).

A similar device for heat detection has already been developed by Kohler et al. [27]. They have developed a system called *Anemon*, that combines vaginal temperature and activity measurements for more accurate prediction of heat. The system consists of two devices, one mounted onto the collar and the second one inserted into the vagina. They gain a detection rate of 90%.

2.4 Data Transfer

For data transfer or sending a calving alarm to the supervisor, a communication module will be needed. For this purpose a GSM module is the best choice. The farmer using such a sensor has to ensure, that the grazing land is covered by GSM cells.

Three different GSM modules (*SIM548* of SimCom, *GE865* of TELIT, and *LEON-G200* of u-blox) have been compared concerning size, power consumption, price, pin count + layout, and availability. LEON-G200 of the swiss company u-blox lists best properties and has the lowest price above 50 pieces. It also features easy coupling with an u-blox GPS module, allowing the use of Assisted GPS for faster positioning.

2.5 Positioning

Outdoor positioning has become very easy since GPS. The electronic device only needs a GPS receiver and a position with an accuracy of several meters (depends on satellites used and obstacles) can be determined. Another possibility is to use cellular networks (GSM) [28, 29]. According to [29] GSM cell size can be up to 35km in rural areas, what results in very low position accuracy. The location of Base Stations of the cellular network have to be known a priori to calculate a position, what results in additional effort. Also a network of smaXtec Base Stations could be used to calculate the position, what would increase the costs for larger areas.

Positioning via cellular network can be realized with the implemented GSM and 433MHz interfaces. For the simple and more accurate way of global navigation satellite positioning, a suitable GPS module has to be selected. Small size GPS chips (by e.g. Broadcom, u-blox, Maxim, Texas Instruments, Atmel, and CSR) have not been available for low volume customers ($<$ 10000 pieces per year). So different GPS modules have been compared concerning power consumption, size, supply voltage, interfaces, pin count + layout, price, availability. Products from u-blox, Telit, and Fastrax have been reviewed. Again the u-blox devices *NEO-6* and *MAX-6* showed good properties and because the u-blox GSM module has already been selected, again an u-blox product has been taken. The smaller version *MAX-6* has currently been under development, so the *NEO-6* module is used. With the u-blox GSM and GPS modules, one is able to easily implement their A-GPS feature *AssistNow* [30].

2.6 System Considerations

Discussing the implementation of the functions mentioned above, brings up different possibilities and problems that have to be considered.

2.6.1 Stand-Alone Sensor

The first idea of a Calving Detector for cows out at pasture is stand-alone vaginal sensor containing devices for temperature and acceleration (freefall) measurements. To find out the position of the cow also a GPS module has to be assembled and for communication with the calving supervisor also a GSM module (including a SIM card) has to be placed onto the hardware.

Some problems come up during considering this solution. Searching for different GSM and GPS solutions showed that such modules will not meet the size constraints for a vaginal sensor. The smaXtec pH Bolus has an outside diameter of $d = 30$mm and the new Calving Detector should be mounted into the same housing. The signal strength in the cow's body will decrease for both modules and positioning or communication cannot be assured anymore. Maybe calving detection can only be done when the sensor drops out of the cow and that might be already too late for obstetrical assistance. Therefore this approach is not further considered.

2.6.2 Mobile Base Station

A second approach for a calving detection system is to place a smaXtec Base Station powered by battery (coupled with solar panel for charging) on the grazing land. The Base Station would represent the center of a fenced area where pregnant cows are allowed to move. The maximum radius of the area depends on the signal strength between sensor and Base Station. A Base Station must have a GSM or an UMTS module to be able to communicate with the calving supervisor. The coverage area could be increased by using more mobile Base Stations.

Before starting further discussion on this idea, a signal strength test between the sensor and a Base Station has to be performed to measure the coverage area of the system.

Signal Strength in Open Area

This test has been performed at a free field in the south of Graz next to a street. Figure 2.1 shows the test setup. The Base Station has been situated at a fixed position and mounted onto a tripod in a height of 1.5m. A rod antenna (*AUREL AS433* Vertical Type Antenna) has been mounted onto the Base Station housing and connected to the first antenna input. A styrofoam plate (height of 3cm) with a compass rose has been used to place the sensor into a defined horizontal and vertical position. The measurement has been done by connecting the Base Station via Ethernet to a laptop and extracting the RSSI values from the received packages. The signal strength has been averaged over 20 samples and then converted into a value in dBm according to the code snippet stated and described in [31]. RSSI values have been collected for steps in azimuth angle of 30° for far distances and 90° at closer positions. By azimuthally rotating the sensor, a rotation of the Base Station around the sensor has been simulated. By rolling the sensor in steps of 90° (0°, 90°, and 180°), further sensor positions have been simulated. With these measured RSSI values, the system with the sensor in the

center has been analyzed and the signal strength for Base Station positions around the sensor can be given.

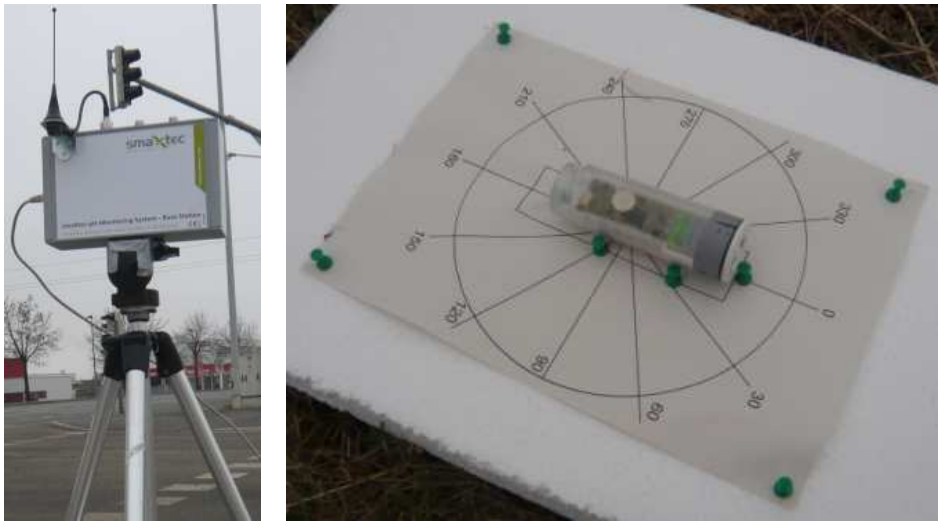

Figure 2.1: Test setup for open area test of smaXtec pH Bolus and Base Station. The left picture shows the Base Station with the connected rod antenna and the Ethernet cable. The right picture shows the smaXtec pH Bolus on a styrofoam plate with a compass rose for aligning the sensor.

The test results in figure 2.2 show, that sufficient signal strength values of $rssi > -95$dBm can only be gained within a radius of 30m. So a calving sensor system with one central Base Station would limit the grazing land for pregnant cows to a very small area. By utilizing all antennas of the a Base Station or using even more Base Stations, not only the coverage area can be increased, but also the setup costs for the farmer will increase. Furthermore, this test only shows signal range for sensors on the ground. For communication with a sensor in the vagina the cow needs to be much closer to the Base Station. Therefore mobile Base Stations are not suitable for calving detection.

2.6.3 Repeater on Collar

Because of the bad signal range of the sensor - Base Station system, it was tried to bring the Base Station functionality as close to the sensor as possible. The best way to place electronic devices on cows is to mount them on a collar. The size constraints are not as strict as for the vaginal sensor, so GPS and GSM modules can be applied onto the hardware.

For this system again communication from vaginal sensor to the collar has to be ensured. So a second test has been performed at the Agricultural Research and Education Centre (AREC) Raumberg-Gumpenstein in Austria.

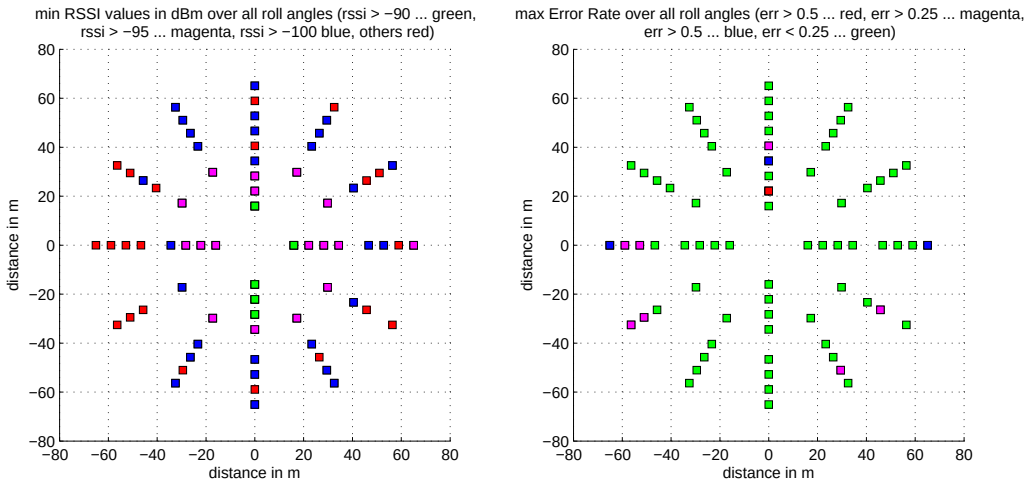

Figure 2.2: Signal strength between sensor and Base Station in open area with the sensor in the center for different Base Station positions. The sensor antenna is situated in the direction of the positive y-axis. The left graph shows the measured signal strength and the right graphs the error rates for positions around the sensor.

Signal Strength within Vagina

A smaXtec pH Bolus has been placed into a cow's vagina by the veterinarian Dr. Johann Gasteiner. Both antenna alignments (geared towards the head first and then towards the tail) have been tested. A coax cable of 5m (*Huber+Suhner RG 223U* 50 Ω and attenuation of $0.36\frac{\text{dB}}{\text{m}}$) with a 433MHz rod antenna (*AUREL AS433* Vertical Type Antenna) at the end has been connected to the Base Station. The Base Station has again been connected via Ethernet to a laptop. The Base Station antenna has been placed on several positions and the RSSI values of the communication between sensor and Base Station have been recorded. This test has been performed using the same software as described in section 2.6.2 reading 20 samples and calculating the mean signal strength. Two significant positions at the cow, where electronic devices can be applied to (pelvis and neck), and two other positions as reference measurements (next to and behind the cow) have been tested. Figure 2.3 shows the test results.

Communication with antenna at the pelvis is possible with the currently used rod antenna. Signal strength with at the neck (−100dBm) is very low but might be increased by using antennas with more suited propagation characteristics.

2.7 Solution

After analyzing the outcome of both tests and discussing the three different approaches, it has been decided to start developing the system with a vaginal sensor and a repeater on the collar as described in section 2.6.3. The lower signal strength measured during the vaginal

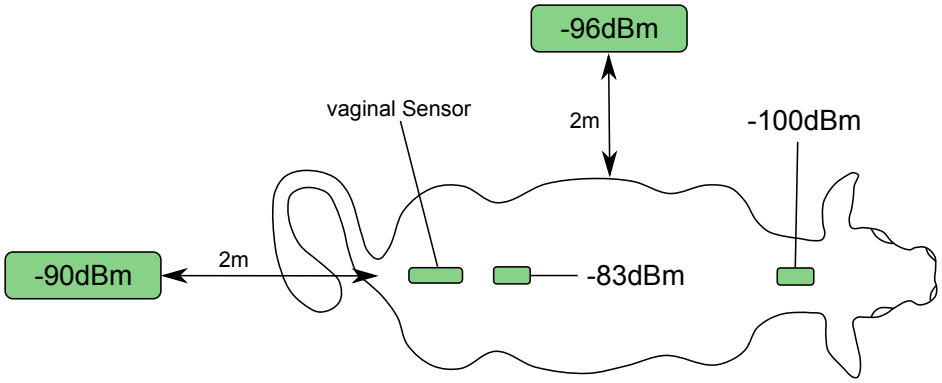

Figure 2.3: Signal strength between sensor and Base Station with sensor in the vagina. Signal strength did not vary much between sensor antenna geared towards head or tail

test (see section 2.6.3) is neglected for now, with the assumption, that RSSI will increase with more suited antennas.

The repeater comes with GSM + GPS modules and communicates via a 433MHz interface with the sensor. The sensor will be able to measure temperature and acceleration. Both, repeater and sensor, will be integrated into the smaXtec system, but will also work without a Base Station. With this solution a wide area (compared to the system with mobile Base Stations) can be covered at lower costs and independent of a smaXtec Base Station.

The next chapter describes the development of hardware and firmware for both, sensor and repeater.

3 Developed System

As mentioned before the newly developed system has to be integrated into the smaXtec pH monitoring solution. Therefore, the same 433MHz RF interface has to be used (see section 3.2.1 and 3.3.1) and the correct communication protocol and configuration data needs to be implemented (section 3.2.2 and 3.3.2).

3.1 Overview

The system is divided into two main parts: a Sensor and a Repeater. Figure 3.1 shows an overview of both parts and their implemented devices.

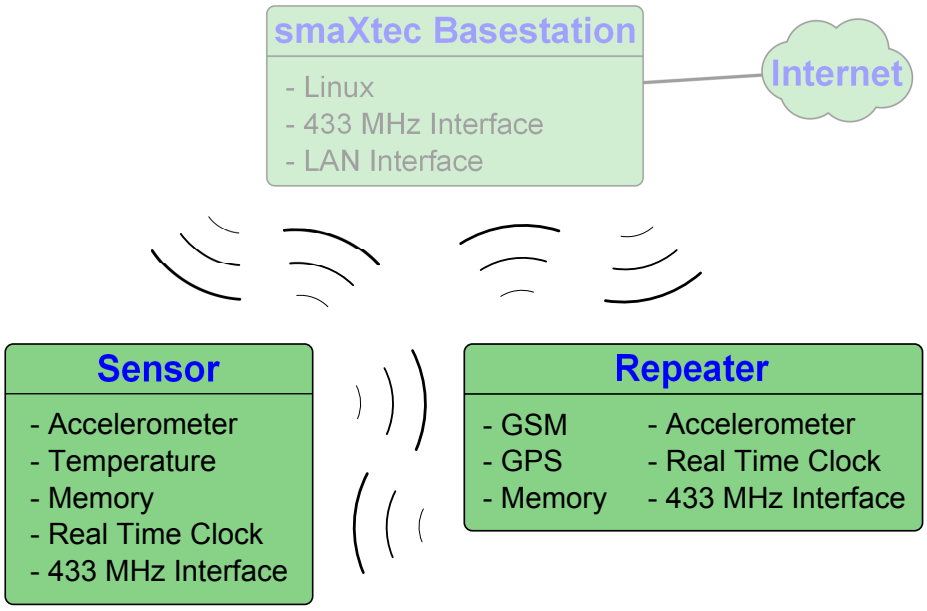

Figure 3.1: Overview of the developed system including a Sensor and a Repeater

Sensor and Repeater must be able to communicate via radio frequency at 433MHz with the smaXtec Base Station and also among each other. It is used for configuration purposes and for data transfer between Base Station, Sensor and Repeater. Both devices are battery powered, so the power consumption has to be kept as low as possible. In the Repeater, which is intended to be mounted at a cow's collar, there is enough space to provide extra batteries to increase lifetime. But the size of the Sensor is constrained. The smaXtec Base Station is

part of the present system. It contains a multi-antenna system (developed by E. Dizdarevic [32] for his master thesis) and an ALIX system board of PC Engines with an UNIX based operating system. On this board operates a program that fetches data from the Sensors and inserts them into a database.

3.2 Sensor

The Sensor is used for temperature and acceleration (free-fall and motion) measurements and intended to be used as *Calving Detector* and *Heat Detector*. To store the measured data for later readouts, the hardware also comes with a real time clock and a memory. The measured data is transmitted on request of a smaXtec Base Station or an equivalent device (smaXtec Mobile Reader or the Repeater described in section 3.3).

The two following sections describe hard- and firmware of the Sensor and discuss the devices used in detail.

3.2.1 Hardware

Figure 3.2 shows a block chart of the Sensor hardware. It comes with four peripherals for data acquisition (accelerometer, ADC), data storage (EEPROM) and a processing unit with a RF interface. The hardware is battery powered and runs on 3.3V.

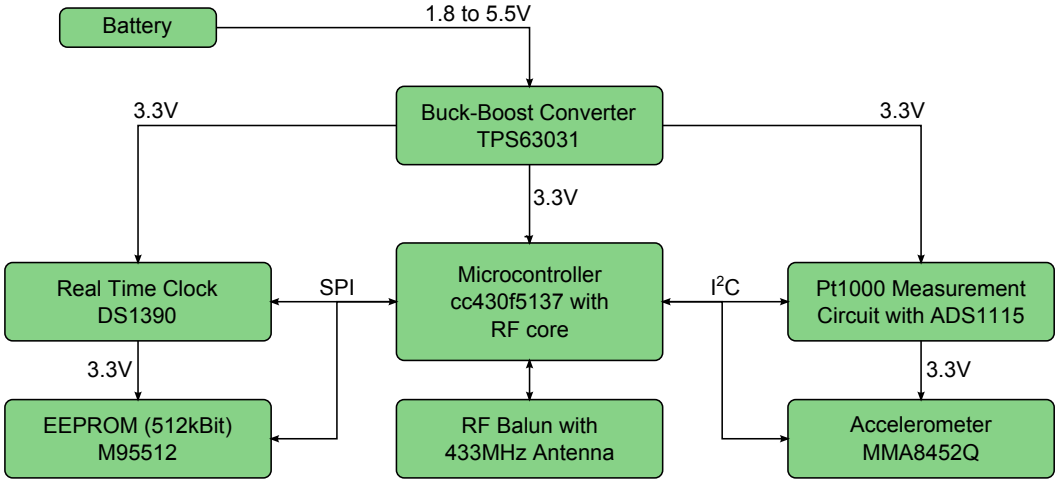

Figure 3.2: Block diagram of the Sensor

Microcontroller

Core of the Sensor hardware is a CC430F5137 microcontroller of Texas Instruments. The CC430 microcontroller series features the MSP RISC CPU + peripherals and also includes

a RF core, what saves a lot of space on the PCB [33]. Table 3.1 gives s short summary of its features.

Supply Voltage Range	1.8V to 3.6V
power consumption in CPU active mode	160μA/MHz
power consumption in Standby mode (LPM3 RTC Mode)	2μA
power consumption with Radio in RX mode	$\approx$ 15mA
2 16-Bit Timer with 5/3 Capture/Compare Registers	
Hardware Real-Time Clock	
2 Serial Communication Interfaces	UART, IrDA, SPI I^2C, SPI
12-Bit ADC with internal and external Reference	
integrated RF Transceiver Core	

Table 3.1: Overview of the features of the microcontroller CC430F5137

Figure 3.3 shows the layout of of the CC430F5137 together with the main peripherals. With its two configurable serial interfaces USCI_A0, USCI_B0 (supporting UART, SPI and I^2C) on Port1 the microcontroller is able to communicate with the external devices (external ADC, Accelerometer, EEPROM and external RTC). The controller is programmable via a JTAG interface, whose necessary lines are connected to a 2x4 pinhead called JTAG. An external crystal X1 is provided to give the microcontroller a precise auxiliary clock.

The RF pins RF_P and RF_N are connected to the balun as recommended in the datasheet (with the according values for 433MHz) and at the end of the balun there is a PCB antenna, developed by FH JOANNEUM in Kapfenberg for smaXtec. For the RF core an external crystal X2 with 26MHz is applied with two load capacitors C20 and C21, which depend on the specifications of the crystal. The load capacitance can be calculated by

$$C_L = \frac{1}{\frac{1}{C_{20}} + \frac{1}{C_{21}}} + C_p \tag{3.1}$$

where C_p includes pin capacitance and PCB stray capacitance and can be typically estimated to be $C_p \approx 2.5\text{pF}$ [33]. With $C_{20} = C_{21}$ and $C_L = 8\text{pF}$ for the crystal NX2520SA of NDK, the resulting capacitance is

$$C_{20} = C_{21} = 2 \cdot (C_L - C_p) = 2 \cdot (8\text{pF} - 2.5\text{pF}) = 11\text{pF} \ .$$

The on-board 12-bit ADC is used for battery monitoring, to be able to detect a low battery voltage. Two precise resistors R7 and R8 (each with $\leq 0.1\%$ tolerance) divide the battery voltage of max 4.2V (Li-Ion Battery) and feed it into an ADC input channel of the CC430. The voltage divider can be switched on and off to avoid unnecessary power consumption. This is done via a discrete highside-switch consisting of T1, T2 and R11 as a pull-up resistor for the gate of the p-channel MOSFET T2.

When the BAT_SENSE_EN outputs a low level, the gate-to-source voltage $U_{GS(th)} = 1.0\text{V}$ (typical) of T1 is not reached, so T1 is off. Therefore, R11 pulls the gate of T2 to the same

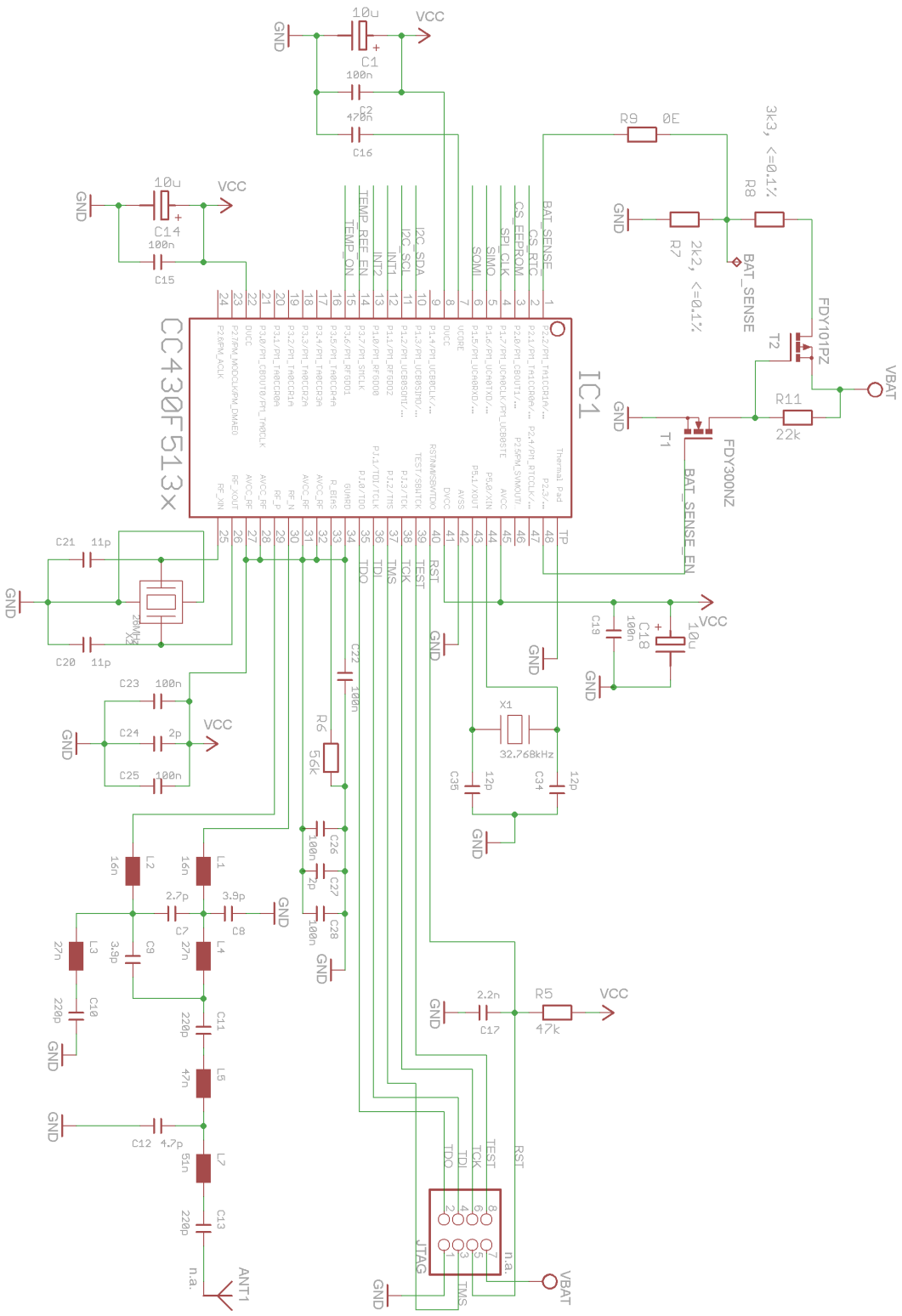

Figure 3.3: Layout of the microcontroller CC430F5137 with RF part

level as its source and T2 is also disabled. When the BAT_SENSE_EN outputs a high level, U_{GS} of T1 exceeds the threshold voltage and pulls the gate of T2 to ground. T2 is now enabled and current runs through the voltage divider R7 and R8.

The internal reference voltage generator of the CC430 provides 1.5V, 2.0V and 2.5V. With a 2.0V reference, battery voltage up to $U_{BAT(max)} = 5\text{V}$ can be measured (see equation 3.2)

$$U_{BAT(max)} = U_{ADC(max)} \frac{R7 + R8}{R7} = 2.0\text{V} \frac{2k2 + 3k3}{2k2} = 5\text{V} \tag{3.2}$$

where 1 LSB of the ADC represents a voltage change ΔU_{BAT} of

$$\Delta U_{BAT} = \frac{U_{ref}}{ADC_{max}} \frac{R7 + R8}{R7} = \frac{2.0\text{V}}{2^{12}} \frac{2k2 + 3k3}{2k2} = 1.221 \frac{\text{mV}}{\text{bit}}$$

which is sufficient to detect low battery voltage. With the highest possible resistor mismatch of R7 and R8 (R7+0.1%, R8−0.1%), an error of 5.992mV will arise what can be considered as negligible low.

All other capacitors are placed for decoupling purpose of the CC430F5137 and its RF core. The layout for the radio and antenna part is taken from the device datasheet in [33].

Power Management

The Sensor hardware operates at 3.3V generated by a buck-boost converter from a typical battery input voltage range. Figure 3.4 shows the schematic overview of the power management.

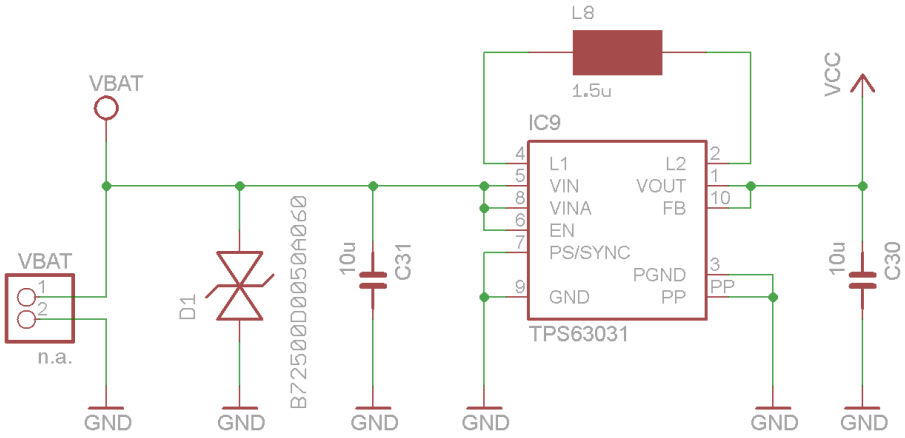

Figure 3.4: Schematic of the power management for the Sensor hardware

In the smaXtec pH Bolus (with a TPS61201 boost converter of TI) some noise at the RF antenna in the range of multiples of the switching frequency has been experienced. Therefore, a different switched regulator for future testing has to be used to generate the 3.3V. Several

buck-boost regulators of Texas Instruments have been compared concerning all necessary parameters and the TPS63031, a fixed output voltage DC/DC converter for 3.3V, is used as its specifications fit best into the requirements. Table 3.2 shows some of its main parameters.

Input voltage	1.8V to 5.5V
Output voltage	3.3V fixed
Output current @ step down mode	800mA
Output current @ boost mode	500mA
Quiescent current	$< 50\mu$A
Efficiency at 1mA to 20mA	90%
Size (10-Pin QFN)	2.5x2.5mm^2

Table 3.2: Parameters of the buck-boost converter TPS63031

By connecting the pin PS/SYNC to GND, power save is enabled which results in higher efficiency for low loads (approximately 25mA peak output current during RF transmit mode is expected). The inductor L8 with 1.5μH is recommended by TI. The EN pin (device enable) and VINA pin (supply voltage for control stage) are permanently connected to VIN, but could have been used to protect a Li-Ion battery against overdischarge. A voltage supervisor connected to the EN pin or a voltage divider on the VINA pin (device shuts down at VINA = 1.5V typical) would prevent drawing current out of a low voltage Li-Ion battery. The ceradiode D1 protects the input against ESD impulses. Its maximum working voltage is at 5.6V. The recommended capacitors C30 and C31 are inserted to improve the transient behavior (see datasheet of the TPS63031 [34]).

Accelerometer

For the purpose of detecting a free-fall event and for recording the animal's activity, an accelerometer with an on-board data processing and a digital interface is necessary to avoid data acquisition on the microcontroller, what would increase the overall power consumption of the Sensor. So an autonomous accelerometer has to be found, that continuously measures acceleration and can inform the microcontroller when a free-fall has been detected. After comparing some devices concerning low power, digital interface and data processing, the MMA8452Q of Freescale Semiconductors is used (see [35] for datasheet). In table 3.3 relevant parameters of the accelerometer are listed. A free-fall detection algorithm is one of four implemented algorithms in the MMA8452Q. More on the settings of this algorithm can be found in section 3.2.2.

Figure 3.5 shows the external parts and the interface of the MMA8452Q. It is connected via I^{2}C bus to the microcontroller. Two pull-up resistors R1 and R2 have to be applied to both lines according to the I^{2}C specifications. The input pin SA0 defines the LSB of the I^{2}C device address. Decoupling capacitors C4 and C6 as well as the bypass capacitor C5 are placed as recommended in the datasheet. Both interrupt lines INT1 and INT2 are directly connected to the microcontroller.

Supply voltage	1.95V to 3.6V
interface voltage	1.6V to 3.6V
Full scale range	±2g/±4g/±8g
Resolution	8bit/12bit
Data rate	1.56Hz to 800Hz
Current Consumption	14μA @ 50Hz
Size (16-Pin QFN)	3x3mm^2
I^{2}C Interface	
2 configurable Interrupt Lines	

Table 3.3: Parameters of the digital accelerometer MMA8452Q

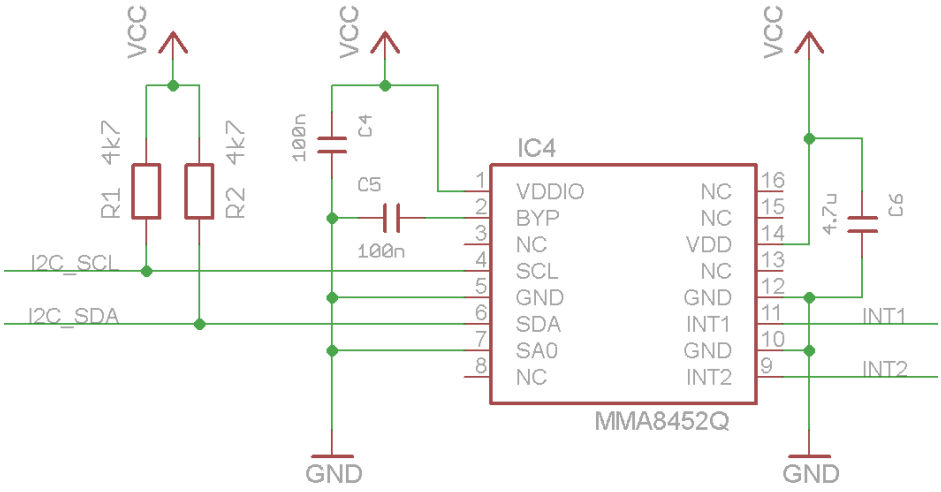

Figure 3.5: Schematic of the accelerometer

Temperature Measurement

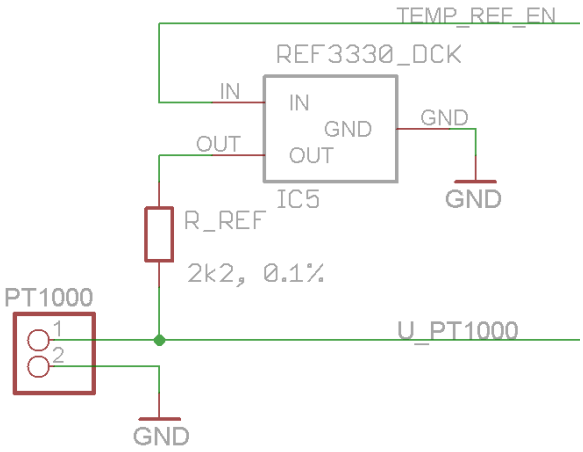

Figure 3.6: The Pt1000 voltage divider with a 3.0V voltage reference

For the temperature measurements, a Pt1000 resistor in a voltage divider with a reference resistor and a 3.0V voltage reference are used (see figure 3.6), like it is also implemented in the pH Bolus of smaXtec. The voltage reference REF3330 (see [36] for datasheet and table 3.4 for main parameters) is enabled and disabled via the microcontroller by simply connecting the input pin of the voltage reference to an output pin of the microcontroller. The voltage divider draws about 1mA, which does not affect the microcontroller (maximum total current for all digital outputs combined should not exceed ±48mA [33]).

Supply voltage	3.02V to 5.5V
Quiescent current	3.9μA
Accuracy	±0.15%
Sourcing/Sinking	35mA

Table 3.4: Parameters of the 3.0V voltage reference REF3330

A Pt1000 resistor has a positive temperature coefficient and a nominal resistor value of $R_{Pt1000} = R_0 = 1000.0\Omega$ at $T = 0°\text{C}$. For positive temperatures the Pt1000 value can be calculated with

$$R_{Pt1000}(T) = R_0 \cdot (1 + \alpha \cdot T + \beta \cdot T^2) \tag{3.3}$$

where

$$\alpha = 3,9083 \cdot 10^{-3}\ °\text{C}^{-1}$$
$$\beta = -5,775 \cdot 10^{-7}\ °\text{C}^{-2}\ .$$

For negative temperatures a third parameter γ is introduced, which is not of further interest for our temperature range. Table 3.5 lists the Pt1000 values for some temperatures.

Temperature in °C	**Pt1000 value in Ω**
20	1077.93500
25	1097.34656
26	1101.22541
27	1105.10310
28	1108.97964
29	1112.85502
30	1116.72925
35	1136.08306
40	1155.40800
45	1174.70406
50	1193.97125

Table 3.5: Pt1000 resistor value for different positive temperatures

The Pt1000 voltage at the voltage divider in figure 3.6 can be calculated with

$$U_{Pt1000} = U_{ref} \frac{R_{Pt1000}}{R_{Pt1000} + R_{ref}} \tag{3.4}$$

where $U_{ref} = 3.0\text{V}$ and $R_{ref} = 2200\Omega$. From 25°C to 26°C and from 40°C to 41°C a voltage at the Pt1000 of

$$U_{Pt1000}|_{T=25°\text{C}} = 3.0\text{V} \frac{1097.347}{1097.347 + 2200} = 0.998391\text{V}$$

$$U_{Pt1000}|_{T=26°\text{C}} = 3.0\text{V} \frac{1101.225}{1101.225 + 2200} = 1.000742\text{V}$$

$$U_{Pt1000}|_{T=40°\text{C}} = 3.0\text{V} \frac{1155.408}{1155.408 + 2200} = 1.033026\text{V}$$

$$U_{Pt1000}|_{T=41°\text{C}} = 3.0\text{V} \frac{1159.270}{1159.270 + 2200} = 1.035287\text{V}$$

can be measured, what results in a voltage change of

$$\begin{aligned} \Delta U_{Pt1000}|_{\Delta T=1\text{K}} &= U_{Pt1000}|_{T=26°\text{C}} - U_{Pt1000}|_{T=25°\text{C}} \\ &= 1.000742\text{V} - 0.998391\text{V} = 2.352 \frac{\text{mV}}{\text{K}} \end{aligned}$$

at T = 25°C and $\Delta U_{Pt1000}|_{\Delta T=1\text{K}} = 2.261 \frac{\text{mV}}{\text{K}}$ at T = 40°C respectively.

The CC430 microcontroller has only a 12-bit ADC with three internal available reference voltages (1.5V, 2.0V and 2.5V). Using the lowest reference voltage available, the highest possible resolution $Q_{ADC12_{max}}$ can be gained of

$$Q_{ADC12_{max}} = \frac{V_{ref}}{ADC_{max}} = \frac{1.5V}{2^{12}} = 0.366 \frac{\text{mV}}{\text{bit}} \ .$$

1 LSB of the 12-bit ADC results in a temperature resolution of

$$TempResolution_{ADC12} = \frac{Q_{ADC12_{max}}}{\min\left[\Delta U_{Pt1000}|_{\Delta T=1\mathrm{K}}\right]} = \frac{0.366\frac{\mathrm{mV}}{\mathrm{bit}}}{2.261\frac{\mathrm{mV}}{\mathrm{K}}} = 0.162\frac{\mathrm{K}}{\mathrm{bit}} \ .$$

A temperature resolution of $0.156\frac{\mathrm{K}}{\mathrm{bit}}$ for one LSB is too bad for our requirements, because changes in temperature of at least 0.1K have to be detected. Therefore, an external ADC with higher resolution and low power consumption is needed and has been found in the ADS1113/4/5 of Texas Instruments. Table 3.6 gives a short summary of the main parameters and figure 3.7 shows the schematic layout of the analog-to-digital conversion of the temperature. Using the ADS1115 with a single-ended input channel, a higher temperature resolution can be gained of

$$Q_{ADS1115_{max}} = \frac{V_{ref}}{ADC_{max}} = \frac{2.048V}{2^{15}} = 0.0625\frac{\mathrm{mV}}{\mathrm{bit}}$$

$$TempResolution_{ADS1115} = \frac{Q_{ADS1115_{max}}}{min\left[\Delta U_{Pt1000}|_{\Delta T=1\mathrm{K}}\right]} = \frac{0.0625\frac{\mathrm{mV}}{\mathrm{bit}}}{2.261\frac{\mathrm{mV}}{\mathrm{K}}} = 0.028\frac{\mathrm{K}}{\mathrm{bit}} \ .$$

Supply voltage	2V to 5.5V
Full scale range	programmable (±6.144V, ±4.096V, ±2.048V, ±1.024V, ±0.512V, ±0.256V)
Resolution	16bit (differential)
Data rate	860 Samples per sec
Current Consumption	150μA at continuous mode
ADS1113/4	1/1 differential/single ended channels
ADS1115	2/4 differential/single ended channels
I^2C Interface	
Internal Reference Voltage	

Table 3.6: Parameters of the 16-bit analog-to-digital converter ADS1113/4/5

The ADS1115 (see datasheet at [37]) with 4 singled-ended input channels is used for testing purposes. In the schematic all the analog input channels of the analog-to-digital converter are connected to the 2x4 pinhead ADC, where external signals can be connected. For future implementation the ADS1113 (only one input channel) is sufficient. The two pull-up resistors R1 and R2 have already been described in section 3.2.1. C3 is the recommended decoupling capacitance. The resistor R4 represents (as prior mentioned) the reference resistor for the voltage divider with the Pt1000.

The IC8 (TLV2401) is an operational amplifier used as an impedance converter to draw less current from the voltage divider, and therefore reduce errors (differential input impedance of TLV2401 $r_{i(d)} \approx 300M\Omega$). Its VCC line is directly connected to an output pin of the microcontroller to enable and disable the OPA when needed. Measurements have shown,

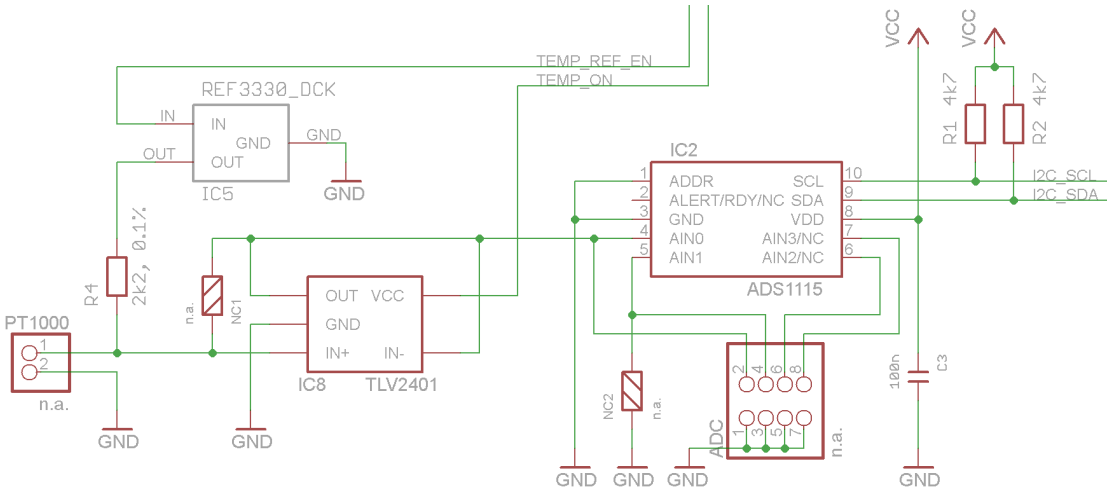

Figure 3.7: Schematic of the temperature measurement with the external ADC

that the error caused by the OPA is greater than connecting the Pt1000 directly to the ADS1115. The ADS1115 has a differential input impedance of $r_{i(d)} = 4.9\text{M}\Omega$ at a full-scale range of $\pm 2.048\text{V}$. The input impedance of the ADC can be considered by adding its value as a parallel resistor to the Pt1000 when calculating the voltage divider.

Having a closer look at the accuracy of all parts used for the analog-to-digital conversion (voltage reference, reference resistor, Pt1000, length of Pt1000 wires, ADC gain match, ADC quantization), there could arise an error of up to 1.5K. Therefore, a single-point error correction in firmware is introduced using a precise reference resistor instead of the Pt1000 (see section 3.2.2).

Memory

To store measured data on the Sensor, a 512kBit EEPROM with SPI bus interface is applied onto the Sensor PCB. The M95512-W of STMicroelectronics only consumes 5μA in standby mode and its supply voltage ranges from 2.5V to 5.5V. It only needs two peripheral devices (see figure 3.8). The pull-up resistor R10 on the chip-select line ensures that the device stays in standby mode whenever the microcontroller pin is in high impedance. Decoupling capacitor C32 ensures a stable supply voltage for the device (see datasheet [38] for more information). The M95512 SPI interface is directly connected to the microcontroller's SPI lines and the chip-select $\overline{\text{CS}}$ is controlled via an output pin of the microcontroller.

Real Time Clock

A real time clock is necessary for the Sensor to map measured data onto a defined date. Although the CC430F5137 comes with an integrated real time clock, an external RTC DS1390U-33 of Maxim Integrated Products (see [39] for datasheet) is placed onto the PCB because the

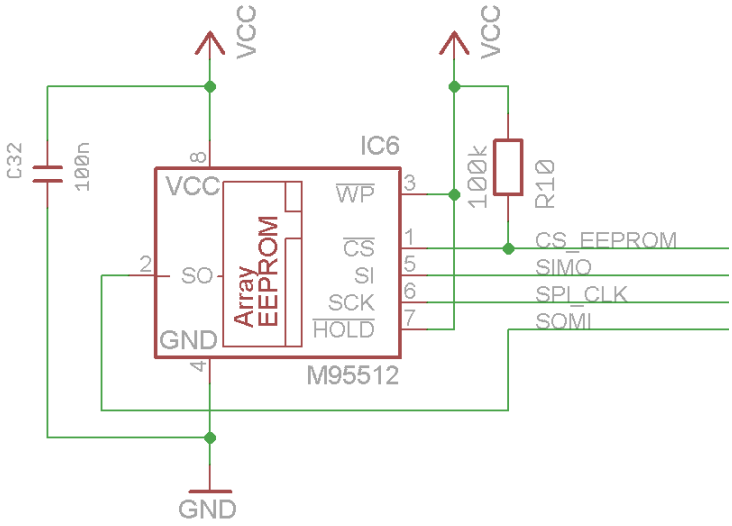

Figure 3.8: Layout of the 512kBit EEPROM M95512-W

microcontroller's internal clock cannot be powered by a backup battery, and therefore loses its date and time when not running. The DS1390 is also used in the pH Bolus of smaXtec. Figure 3.9 shows the layout of the RTC. For future use (with fixed battery) the DS1390 will be removed.

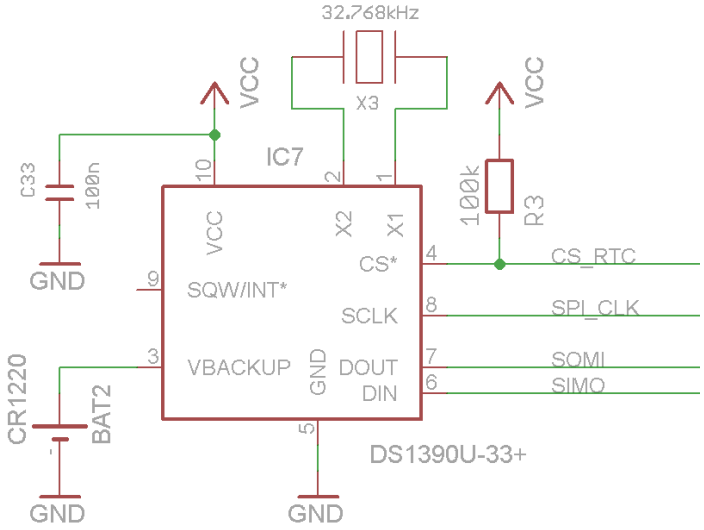

Figure 3.9: Connection of the real time clock DS1390U-33

The DS1390U-33 has a SPI interface and is (together with the EEPROM mentioned above) connected to the microcontroller's SPI lines. An external backup battery (CR1220 with 3V and 40mAh) is connected to the DS1390. If the Sensor is powered off (no external battery applied to the VCC lines of the Sensor PCB), the RTC automatically switches to the backup

battery and sinks $I_{BACKUP_{max}} = 1\mu A$. So the CR1220 is able to keep the backup voltage for at least

$$t = \frac{BatCapacity}{I_{BACKUP_{max}}} = \frac{40\text{mAh}}{1\mu\text{A}} = 40,000\text{hours}$$

or more than 4.5years. An external quartz crystal X3 with 32.768kHz has to be applied for the DS1390 and again pull-up resistor R3 for the chip-select line and decoupling capacitor C33 are placed onto the Sensor PCB.

3.2.2 Firmware

The firmware of the Sensor is designed to keep the microcontroller as long as possible in low-power mode to hold the power consumption caused by the CC430 as low as possible. Enabling the RF core causes the highest power consumption, and therefore this is done very rarely and only for short time. Measurements are also performed only once in a while to save energy.

Main State Machine

The infinite-state machine in the main loop has three states: **SLEEP**, **READY** and **SELECTED**. Figure 3.10 shows the chart of the main state machine. It is coupled with the Timer A0 that causes the state transitions after predefined timeouts. The firmware mainly stays in **SLEEP** mode, where the controller is set into low-power mode LPM3 (only draws 2.0μA). It gets woken up by interrupts of the Timer A0 or by external interrupt signals coming from accelerometer's INT1 and INT2 lines connected to Port1.

The microcontroller wakes up from LPM3 under the following conditions:

- When the wake-up event has been generated because the *Communication Interval* is over, the controller is set into **READY** state and the radio core is set into receive mode. Whenever the Sensor receives a correct command, the *Communication Timeout* is retriggered and extended to another 3000msec. If the Sensor receives the *Select* command, it changes its state to **SELECTED** and further commands can be performed (see following subsection *Message Interpreter* for further details).
- When a *Measurement Interval* is over, the controller performs the temperature measurement and also finishes the analysis of the acceleration data. Both values together with a timestamp are then stored into the EEPROM and the controller is set back to low-power mode.
- Whenever new data of the accelerometer is available, the controller leaves the low-power mode and starts reading and processing the data. This is described in the following subsection *Accelerometer*. Measurements and data processing is only done in **SLEEP** state.

Table 3.7 lists the default values used for the intervals and timeouts. If the accelerometer has detected a freefall event, the Sensor has been expelled from the vagina. At this point, the Sensor sets the communication interval to $T_{CommunicationInterval} = 2\text{sec}$, what means that the Sensor stays in receive mode and is continuously listening for received data, and therefore can respond to the next inventory with lowest possible delay. After the Sensor has been read, the *Communication Interval* is reset to its predefined value.

Description	**Value**
$T_{MeasurementInterval}$	60sec[1]
$T_{CommunicationInterval}$	15sec[2]
$T_{CommunicationTimeout}$	3000msec

[1] only for testing purposes. In operation this value will be around 300sec ($\widehat{=}$5min).
[2] only for testing purposes. In operation this value will be around 600sec ($\widehat{=}$10min).

Table 3.7: Intervals and timeouts for the main state machine

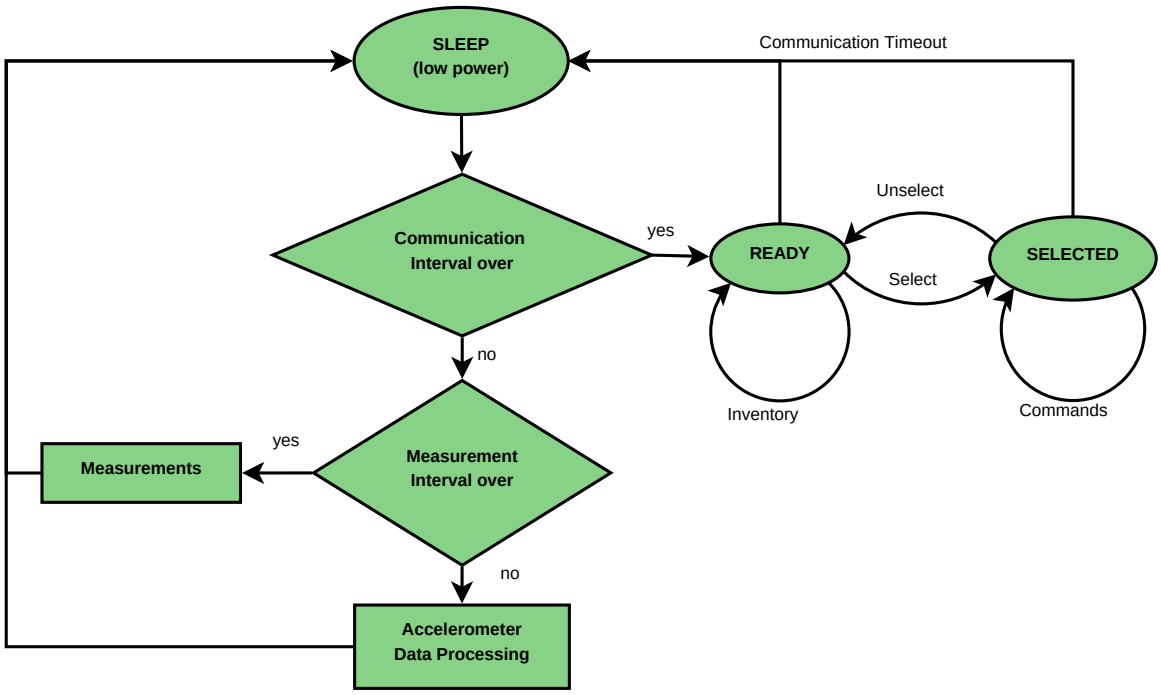

Figure 3.10: State chart of the Sensor firmware

Message Interpreter

Received data via the radio is immediately interpreted and the radio core is set to transmit mode to send back the correct response. The format of received messages has been described by G. Zancolo in his master thesis [40]. Table 3.8 gives a short overview of the commands used for communication. The first four commands *Inventory*, *Select*, *Quiet* and *Animal*

Inventory are the only ones that can be interpreted while the Sensor is in the **READY** state. Before sending other commands, the Sensor has to be set into the **SELECTED** state, which is done with the *Select* command.

One new command is introduced to be able to run an inventory on one animal only, the *Animal Inventory*. With this command the Repeater or any Base Station is able to contact the Sensors applied to one specific animal.

Command	"AI" (0x41 0x49)
Parameter	Current Round (1 Byte $\neq$ 0x00) Animal ID (16 Byte)
Response	Animal ID (16 Byte) Serial Number (8 Byte) Inventory Status (1 Byte)

Command	**Id**	**Description**
Inventory[3]	"I"	With an Inventory a Base Station looks for Sensors in its surrounding
Select[3]	"S"	Sets a Sensor to the **SELECTED** state
Quiet[3]	"-"	Tells the Sensor not to answer further Inventories with the last Inventory Round Number received
Animal Inventory[3,4]	"AI"	Runs an Inventory Round on a specific animal
Unselect	"U"	Sets the Sensor from **SELECTED** back to **READY** state
Erase Data	"X"	deletes data from Sensor
Query Data	"Q"	returns the number of data available
Read Data	"R"	reads the given amount of data
Flash Read	"FR"	reads the flash configuration
Flash Write	"FW"	writes the flash configuration
Set Time	"T"	sets date and time of the real time clock
Get Time	"M"	gets date and time
Get Version	"V"	returns the protocol version string specified in the Sensor's firmware
Get RSSI	"A"	returns the Sensor's last measured RSSI value
Reset	"Z"	restarts the Sensor

Table 3.8: Overview of the commands that can be interpreted by the Sensor

[3] These are the only commands that can be interpreted while the Sensor is in the **READY** state.
[4] This is a new command developed for communication between Repeater and Sensor that belong to the same animal.

Accelerometer

The freefall detection algorithm inside the MMA8452Q checks the acceleration values of all three axes and compares them with a user definable threshold (FF_MT_THS Freefall and Motion Threshold Register). If all values are underneath the threshold for a defined amount of time (FF_MT_COUNT Debounce Register), the freefall interrupt is raised and sent to the microcontroller. The debounce time depends on the data rate of the MMA8452Q (ODR = 50Hz is chosen). Using a constant acceleration for gravity on earth of $a = 9.807\frac{\mathrm{m}}{\mathrm{s}^2}$ and a starting velocity of $v(0) = 0$, the freefall height can be calculated with

$$v(t) = \int a\ dt = a\ t + v(0) = a\ t \tag{3.5}$$

$$s(t) = \int v(t)\ dt = \int a\ t\ dt = a\ \frac{t^2}{2} + s(0) = a\ \frac{t^2}{2}\ . \tag{3.6}$$

Expecting the Sensor to be in freefall for about 1m, the time in freefall is

$$t_{\text{freefall}} = \sqrt{\frac{2\ s}{a}} = \sqrt{\frac{2 \cdot 1\text{m}}{9.807\frac{\text{m}}{\text{s}^2}}} = 451.6\text{ms}$$

and using the accelerometer at a datarate of ODR = 50Hz, the (FF_MT_COUNT) debounce register has to be set to

$$\text{FF\_MT\_COUNT} = \frac{\text{ODR}}{t_{\text{freefall}}} = \frac{50\text{Hz}}{0.452\text{s}} = 111\ .$$

This theoretical value should be reduced to a lower value in operation, but these settings will be adapted after reference data has been collected and analyzed. A data rate of ODR = 50Hz is used, because the MMA8452Q has a low power consumption of 14μA and still a high sample rate. The next sample rate would be 12.5Hz, what results in a rather high measure period of $80ms$.

Recording the movement with the accelerometer is done by setting its data rate to 12.5Hz and reading the xyz-values whenever new data is available. The data ready interrupt of the MMA8452Q triggers the selected interrupt line and the microcontroller reads the registers after it has been raised. To remove the 1g offset of the device, the high-pass filter inside the accelerometer is used with a cutoff frequency of 0.125Hz. To reduce noise on the data, the 2 LSBs are removed (using 10bit instead of 12bit) and a FIR low-pass filter with three coefficients is applied (using five or more coefficients already causes a much higher computing time). The absolute values of each axis are then summed up. After one measurement interval a movement index a_{idx} is calculated with

$$a_{idx} = \frac{1}{n}\sqrt{\left(\sum_{i=0}^{n}|a_x|\right)^2 + \left(\sum_{i=0}^{n}|a_y|\right)^2 + \left(\sum_{i=0}^{n}|a_z|\right)^2} \tag{3.7}$$

where n is the number of samples used in the calculation process and a_x, a_y and a_z are the filtered acceleration values of each axis (where 1 LSB equals 1.953mg). Figures of the movement index can be found in chapter 4.

Temperature Measurement

Before starting the measurement, the voltage reference REF3330 and the TLV2401 are enabled via two controller output pins connected to the device's VCC lines. After waiting 150ms (to ensure stable supply voltages), the ADS1115 conversion is started. During communication via I^2C with the external ADC, the interrupts of the accelerometer are disabled to avoid errors due to interaction with both devices at the same time (accelerometer readouts are done in the ISR).

The ADS1115 has two modes of operation: continuous and single-shot mode. In continuous mode it runs conversion with a pre-definable sample rate. In single-shot mode the ADC enters power-down mode after the conversion is finished. The complete configuration is done via a 16bit config register, where conversion mode, data rate, full scale range and the input multiplexer can be selected. To measure the voltage at the Pt1000, the ADS1115 is set into continuous mode at a datarate of 860 samples per second with a full scale range of 2.048V and 10 samples every 2ms are read. Afterwards it is set back to power-down mode again. Using the mean value over these 10 samples the Pt1000 voltage is calculated with

$$U_{Pt1000} = \frac{\sum_{i=1}^{10} AdcSample_i}{10} \; \frac{V_{ref}}{ADC_{max}} = \frac{\sum_{i=1}^{10} AdcSample_i}{10} \; \frac{2.048\text{V}}{2^{15}} \; .$$

The ADS1115 is a 16bit ADC for differential input signals, but only the positive input range is used. Therefore, one bit is lost and the maximum resolution is $ADC_{max} = 2^{15}$. The Pt1000 value can further be computed to

$$R_{Pt1000} = \frac{U_{Pt1000}}{U_{ref} - U_{Pt1000}} \; R_{ref} \; .$$

All electronic devices have a certain inaccuracy that has to be considered by a temperature error correction. This is done by a single-point calibration where a accurate reference resistor $R_{Pt1000(ref)}$, which resistor value is close to the value of a Pt1000 at the common operating temperature (see table 3.5 for some resistor values), is connected instead of the Pt1000 and a correction factor $k_{tempCorr}$ is calculated with

$$k_{tempCorr} = \frac{R_{Pt1000(ref)}}{R_{Pt1000(measured)}}$$

and using this factor, the calculation of the Pt1000 value is corrected to

$$R_{Pt1000} = k_{tempCorr} \cdot R_{Pt1000(measured)}$$

The temperature can now be calculated using equation 3.8.

$$T = -\frac{\alpha}{2 \cdot \beta} - \sqrt{\frac{\alpha^2}{4 \cdot \beta^2} + \frac{R_{Pt1000} - R_0}{\beta \cdot R_0}} \tag{3.8}$$

Executing the code of equation 3.8 to calculate the temperature (with $f_{clk} = 1\text{MHz}$) needs up to 100ms. Therefore, a linearization in steps of 1K for the main temperature range is used. The Pt1000 values for temperature values from 15 to 50°C have been pre-computed and stored in an array in the Sensor firmware. The two closest Pt1000 values are looked up in the Pt1000 value array (R_{lBound} and R_{uBound}) with the according temperature for the lower value (T_{offset}) and then a linearization between those two values is performed, what leads to

$$T = T_{offset} + \frac{R_{Pt1000} - R_{lBound}}{R_{uBound} - R_{lBound}} \tag{3.9}$$

This linearization results in a maximum error of 0.037mK at 40°C to 41°C and cannot be seen in the outcome of the measurement.

Battery Monitoring

The internal 12bit ADC of the CC430F5137 with its internal reference voltage generator is used to have the battery voltage monitored. The voltage divider is prior enabled by setting the P2.3 bit and the ADC12 is started in single channel and continuous conversion mode. 10 samples are taken and the mean value is used to calculate the voltage on R_2 with

$$U_{R_2} = \frac{\sum_{i=1}^{10} AdcSample_i}{10} \frac{V_{ref}}{ADC_{max}} = \frac{\sum_{i=1}^{10} AdcSample_i}{10} \frac{2.0\text{V}}{2^{12}}$$

and U_{R_2} is further used to calculate the battery voltage U_{Bat} to

$$U_{Bat} = U_{R_2} \frac{R_1 + R_2}{R_2} = U_{R_2} \frac{2k2 + 3k3}{2k2} \ .$$

The battery voltage can then be used to inform the Repeater (or Base Station) that the battery should be changed or charged soon.

Configuration

To integrate the newly developed Sensor into the present system, its configuration has to look exactly the same as the one of the pH Bolus. Otherwise severe changes in PC software would have been necessary what would have caused a lot of work. Therefore, the Sensor configuration contains several dummy values, that can be remove in future. Table 3.9 shows the main config parameters. The Sensor config also includes some parameters concerning the radio core of the CC430, that allows changing data rate, frequency, etc. But these values are not of further interest. Configuration is done via the RF interface with the previously mentioned commands and has been done with an admin tool developed by smaXtec (used for testing purposes).

name	**bytes**	**description**
channel_nr	1	RF channel number (see CC430 datasheet [33])
sensorType	1	this will be used in future to distinguish between different device types (e.g. pH Bolus, Calving Detector, Heat Detector, Repeater)
serial_nr	8	unique sensor identifier
animal_id	16	each animal has its own ID
comm_interval	2	interval in seconds between communication wake ups
comm_timeout	2	time in milliseconds how long a Sensor waits for a packet to be received over RF
measurement_interval	2	interval in seconds when measurements are executed
temp_corr	4	float value representing the correction factor for temperature measurement

Table 3.9: Main Sensor configuration parameters

Memory and Real Time Clock

All measured data is stored in the EEPROM. To be able to read the data correctly, the same format (as it has been implemented in the pH Bolus of smaXtec) has to be used to store data. One datum consists of 9 bytes

Date and Time					Temp		FF/Acc	
year	month	day	hour	minute	temp1	temp2	acc1	acc2

e.g.

0x11	0x09	0x24	0x13	0x56	24	95	3	27

and they are stored starting at address 0x11 ($\widehat{=}$ 17). This address offset comes from earlier versions of the smaXtec pH Bolus, where the configuration has been stored in the EEPROM. The bytes *temp1* & *temp2* and *acc1* & *acc2* are the integer and the decimal part of the temperature and the movement index, respectively . The example shows an entry for 2011/09/24 at 13:56 with T = 24.95°C and a movement index of 3.27. The amount of available data is stored at address 0x00 and 0x01. With the 512kBit ($\widehat{=}$64kByte) EEPROM and 9 bytes for a datum, there can be stored

$$\left\lfloor \frac{64 \cdot 1024 - 17}{9} \right\rfloor = 7279 \text{ measurements .}$$

The real time clock should be set before the Sensor starts measuring to have a correct time to data mapping. This can be done using the prior described admin tool.

As already mentioned in section 3.2.1, the CC430F5137 has an integrated RTC without a backup battery connection. However, both RTCs (CC430 internal RTC and external DS1390) have been programmed and tested.

Calving and Estrus Detection

The detection of calving and estrus is currently not implemented. Lot of reference data has to be collected to develop and implement the algorithms. But the prior mentioned sources movement, vaginal temperature and freefall (see chapter 1 and chapter 2) can be measured with the implemented devices. Movement and temperature is stored in the EEPROM and also a first-in-first-out buffer in the Sensor firmware is implemented that stores the latest measured values, so that they can be analyzed afterwards.

3.2.3 PCB Layout for Antenna

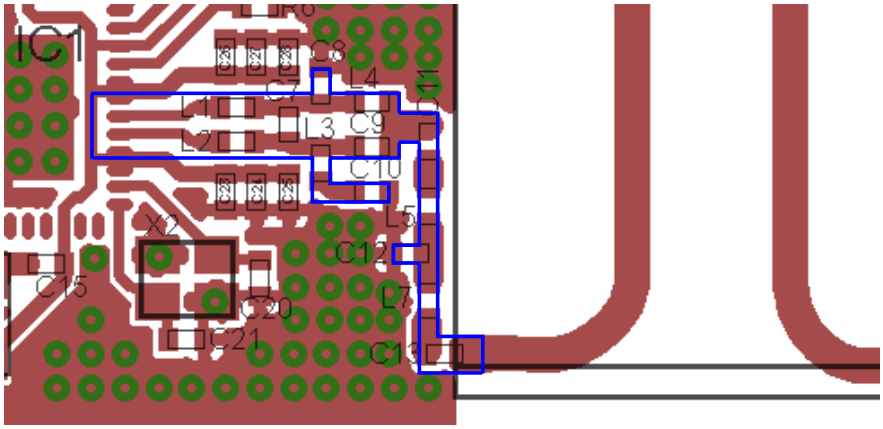

Figure 3.11: The blue marked path shows the converter from differential to single ended load and the antenna matching circuit as recommended by Texas Instruments in [33].

The PCB antenna on the Sensor node has prior developed for the smaXtec pH Bolus. For connecting the antenna to the RF interface of the CC430, the recommended design of Texas Instruments given in [33] is used. Figure 3.11 shows the RF balun containing the converter circuit from differential to single ended load and the matching network for the antenna. Width of the strip lines are taken from measurements done for the smaXtec Base Station antenna path.

3.3 Repeater

The Repeater is developed to communicate with the Sensor described above (or for future purpose with any sensor applied to the animal) and to interact with a human supervisor on specific conditions. It is intended to be mounted on a cows collar. A GPS module is added to fetch the cows position out at pasture and for sending messages (SMS or emails) or upload data via GPRS a GSM module is applied. The two following sections describe hard- & firmware considerations and implementations on the Repeater.

3.3.1 Hardware

Like the Sensor hardware, the Repeater also comes with a real time clock and a 512kBit EEPROM connected via SPI and an accelerometer MMA8452Q connected via I^2C to the microcontroller (see block diagram in figure 3.12). The only difference to the Sensor is, that they share the same Universal Serial Communication Interface (USCI_B0) which is necessary because the GSM module occupies the second one (USCI_A0). These devices have of course been tested, but are currently not in use. For future development and testing purposes they are be quite useful. Nevertheless, it is strongly recommended to separate SPI and I^2C devices and connect them to different IO ports to avoid errors.

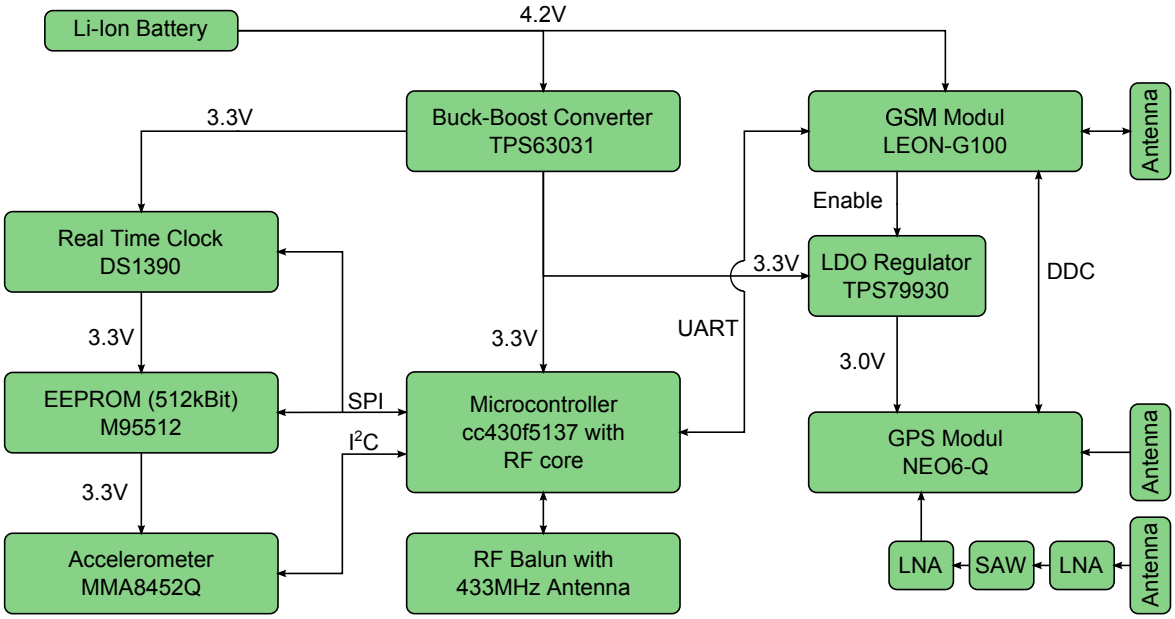

Figure 3.12: Block diagram of the Repeater and its main components

Microcontroller

The core of the Repeater is again a CC430F5137 (see figure 3.13) and it includes the same features like the Sensor, but without the temperature measurement via the extern ADC

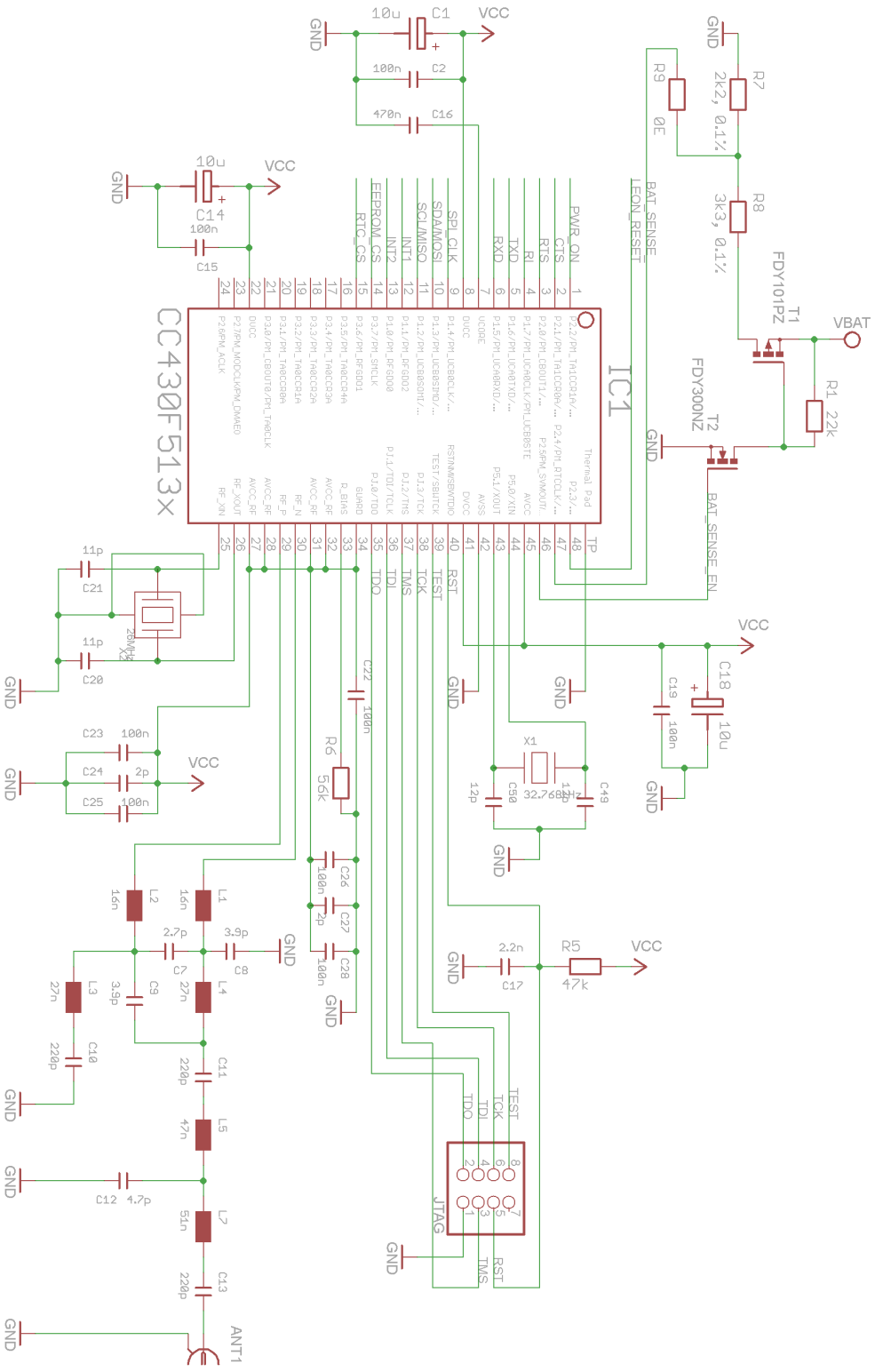

Figure 3.13: Layout of the CC430F5137 microcontroller of the Repeater

ADS1115. In addition a GSM module is connected via UART to the USCI_A0 (RXD and TXD Port1.5 & 6). Also the ring indicator RI and both hardware flow control lines RTS and CTS are connected to the controllers Port1 and Port2. Also two control lines power on (PWR_ON) and reset (LEON_RESET) are attached to input pins of the controller. Details on the GSM module are discussed in the subsection *GSM and GPS Modules*.

The battery monitoring equates the Sensor's circuit, but it is connected to different lines Port2.4 & 5. Also JTAG interface, crystals, RF balun and decoupling capacitors are designed the same way. Instead of the PCB antenna used for the Sensor, a SMA connector is provided on the Repeater to be able to test different antennas concerning their signal strength and range.

Powermanagement

Figure 3.14 shows the layout of the Repeater's power management. It uses the TPS61201 of Texas Instruments, like it has also been used in the smaXtec pH Bolus, to generate the 3.3V out of a Li-Ion battery connected to the hardware (see table 3.10 for the main features or the datasheet [41]).

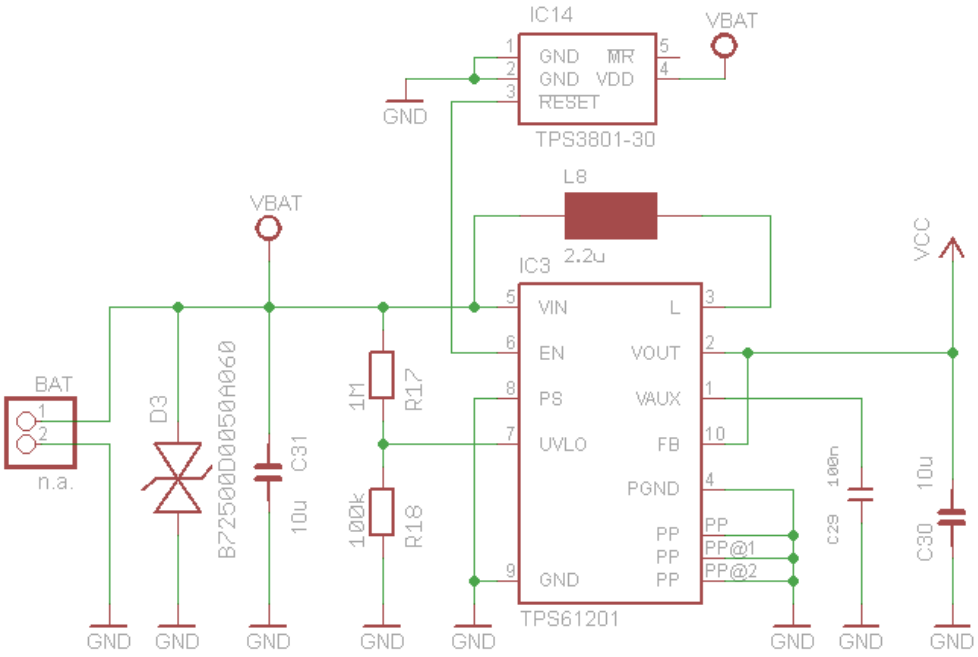

Figure 3.14: Schematic of the power management for the Repeater

For undervoltage protection of Li-Ion batteries, two mechanisms have been implemented and tested. A voltage supervisor TPS3801-30 is applied to protect the battery against undervoltage discharge. Its threshold voltage is at $V_{IT-} = 2.64V$ (see datasheet [42] for further details). The $\overline{\text{RESET}}$ output of the supervisor is directly connected to the EN input

Input Voltage Range	0.3V to 5.5V
Output voltage	3.3V
Quiescent current	55μA
Shutdown current	1.5μA
output current	300mA
Size (10-Pin QFN)	3x3mm^2
Programmable Undervoltage Lockout Threshold	
turn off voltage	250mV
turn on voltage	350mV
Power Save Mode for Improved Efficiency at Low Output Power	

Table 3.10: Overview of the features of the Boost Converter TPS61201

of the voltage regulator. Whenever the input voltage drops below the threshold voltage, the $\overline{\text{RESET}}$ signal is pulled to ground an the voltage regulator is disabled.

A second shutdown mechanism is available using the undervoltage lockout of the TPS61201. With a voltage divider sourced by the battery voltage and connected to the UVLO pin, a lockout voltage can be programmed with equation 3.10, where U_{UVLO} is the undervoltage lockout threshold ($U_{UVLO-} = 250\text{mV}$ for turn off, $U_{UVLO+} = 350\text{mV}$ for turn on).

$$U_{Bat(th)} = U_{UVLO}\frac{R1 + R2}{R2} \tag{3.10}$$

The voltage divider can further be calculated to

$$R17 = \frac{(U_{Bat(off)} - U_{UVLO-})}{U_{UVLO-}}\ R18\ .$$

If the same shutdown voltage as the supervisor of $2.64V$ is desired, the resistors can be computed to

$$R17 = \frac{(2.64\text{V} - 0.25\text{V})}{0.25\text{V}}\ R18 = 9.56 \cdot R18\ .$$

Resistor values R17 = 1MΩ and R18 = 100kΩ are used, what results in voltage thresholds for the battery of

$$U_{Bat(off)} = U_{UVLO-}\ \frac{R1 + R2}{R2} = 0.25\text{V}\frac{1\text{M}\Omega + 100\text{k}\Omega}{100\text{k}\Omega} = 2.75\text{V}$$
$$U_{Bat(on)} = U_{UVLO+}\ \frac{R17 + R18}{R18} = 0.35\text{V}\frac{1\text{M}\Omega + 100\text{k}\Omega}{100\text{k}\Omega} = 3.85\text{V}\ .$$

This means that the applied Li-Ion battery has to be at least at 3.85V, before the controller starts operating and will shut down at 2.75V. This feature prevents the user from applying low charged batteries to the hardware. For testing purposes the UVLO has been disabled by removing R18.

As in the Sensor hardware, again a ceradiode D3 for ESD protection of the power input lines, decoupling capacitors and the recommended inductor are applied.

GSM and GPS Modules

The GSM module LEON-G200 (see [43] for datasheet) and the GPS module NEO-6Q (see [44] for datasheet) of u-blox are chosen, because they fit best the requirements. Its advantageous, that both devices come from the same company, because they are designed to interact with each other. The GPS module can be directly connected to the LEON-G200 via their DDC interface (I^2C compatible) and it is fully controllable by AT commands over the GSM module. More features will be described in section 3.3.2.

LEON-G200 Table 3.11 lists the main parameters of the GSM module and figure 3.15 shows the schematic and the connections to peripherals. The hardware design has been made considering information and hints in the System Integration Manuel [45] and the LEON-G200 datasheet [43].

Input Voltage Range	3.0V to 4.5V
Supply peak current (max)	2.5A
Charging voltage	5.6V to 15V
Charging current	400mA to 1000mA
Backup voltage	1.0V to 2.25V
Backup current consumption	2.0μA
Power consumption in Power Off Mode	$< 90\mu$A
Size (50-Pin)	29.5x18.9mm^2
full quad-band GSM/GPRS data and voice	
full access to u-blox GPS receivers	
UART and DDC interface, 2 GPIOs	
Network Indication	
embedded TCP/UDP stack	
FTP, HTTP, SMTP	
Battery charging	

Table 3.11: Main parameters of the GSM module LEON-G200

The LEON-G200 is connected to the microcontroller with its 4 UART lines (RxD, TxD, RTS and CTS), where TxD and RxD follow the naming convention of modems, so TxD is an input (data to be transmitted) and RxD is an output (data that has been received). With the ring indicator RI connected to the controller, it is possible to detect incoming calls or SMS. If the module is in power off state, it can be switched on by pulling the PWR_ON pin to ground. This pin has high input impedance, and therefore is pulled to VCC via an 100kΩ resistor R11. The reset pin RESET_N has an internal pull-up resistor of 12.6kΩ which pulls the pin to 1.88V when the module is not in reset state. Connecting this pin to the controller, one can either reset the module (pull the LEON_RESET line to ground) or find out if the device is in reset state (reading the input pin LEON_RESET on the controller). L6 and C45 are applied for input protection and filter purpose. The two available input/output pins GPIO1 and GPIO2 are used in their default configured purpose. GPIO1 is connected to the network

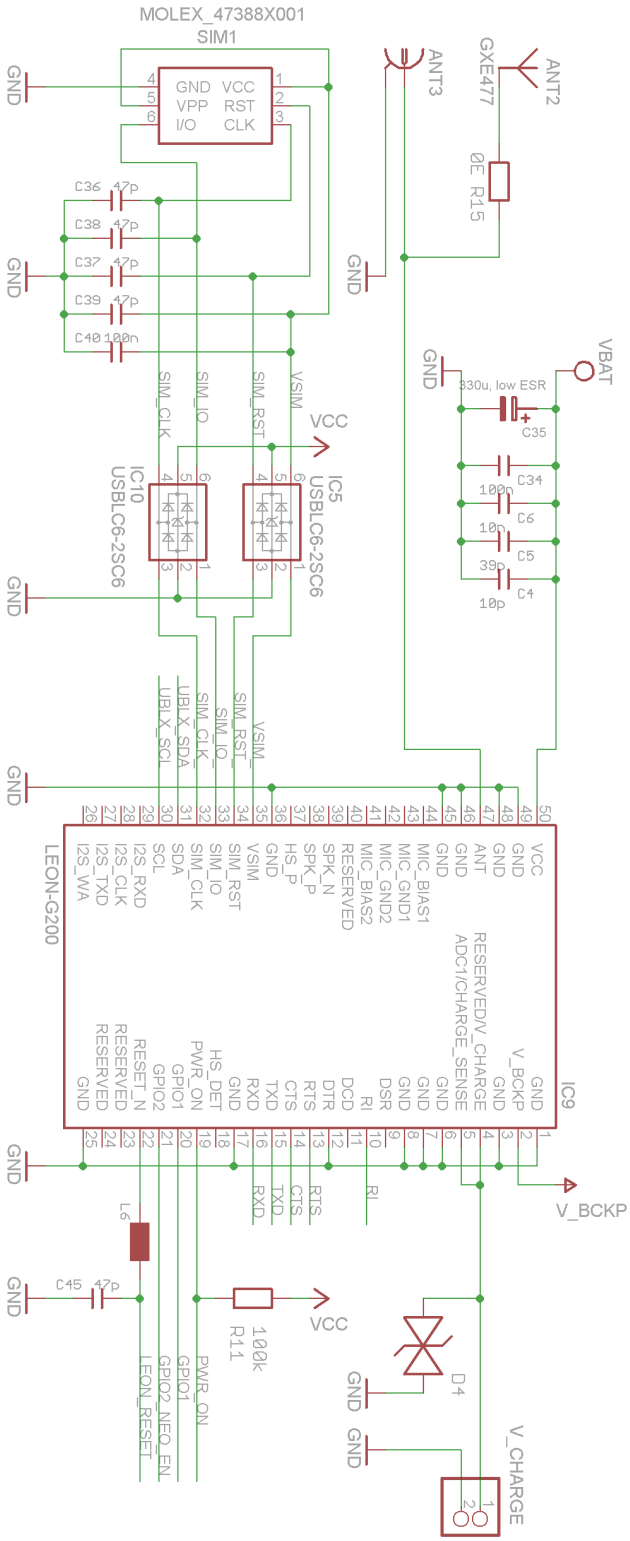

Figure 3.15: Schematic of the GSM module and its peripherals

indication circuit (see figure 3.16) and GPIO2 enables the LDO regulator powering the GPS module (GPIO2_NEO_EN). Both GPIOs can be reconfigured with AT commands. The LEON-G200 and the NEO-6Q are connected via the DDC interface (SDA and SCL). The SIM card connector SIM1 (473882001/3001 of molex) is connected with two low capacitance ESD protection devices USBLC6-2 of STMicroelectronics (see [46] for datasheet) to the four SIM IOs (clock, data, reset and supply output) of the GSM module. Bypass capacitors C36 to C39 and a decoupling capacitor C40 are applied as recommended [45].

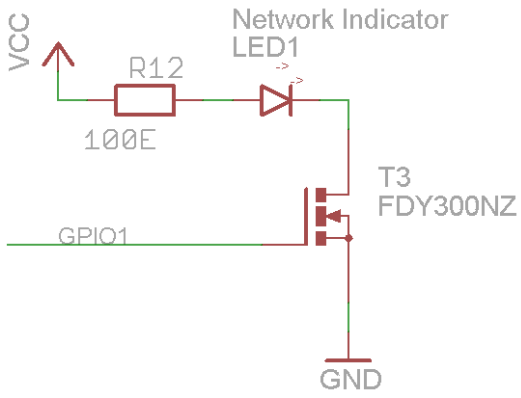

Figure 3.16: Network indicator circuit connected to GPIO1 of LEON-G200

For testing both, an external antenna and a PCB mounted antenna, although signal quality loss by antenna mismatch will be caused, a SMA connector and a ceramic antenna are connected to the antenna I/O pin ANT of the LEON-G200. The ceramic antenna ANT-GXE477 of Round Solutions is a small PCB mounted triband GSM 50Ω antenna suitable for GSM 850 (with matching circuit), GSM 900, GSM 1800 and GSM 1900 (see [47] for datasheet) and fits perfectly onto the hardware. It can be disconnected via a 0Ω resistor from the SMA jack. The PCB layout of the antenna path is discussed in section 3.3.3.

A rechargeable Li-Ion battery (SANYO UR 18650 S) with a continuous discharge current of 10A is used to power the module, so that the maximum current of ICC_PEAK = 2.5A drawn by LEON-G200 can be guaranteed. Five capacitors placed near the VCC pin reduce the voltage ripples. Charging the battery can be done via the V_CHARGE pin by applying a voltage and current limited charger (5.6V to 15V with max 1A). The internal charging algorithm implements a classic Li-Ion battery charging process [45].

The backup voltage pin V_BCKP is used to source the integrated real time clock with a backup voltage (1.0V to 2.25V, 2.0V typ). When the module is powered via VCC, 2.0V are internally generated and output at the V_BCKP pin. If VCC is disconnected from the battery, an external source is applied to the V_BCKP pin to keep the internal RTC running. This is discussed in the following subsection *Backup Voltage for GSM and GPS Module*.

NEO-6Q For positioning of the animals, the GPS module NEO-6Q of u-blox is used. The layout containing antenna connection is given in figure 3.17 and table 3.12 gives an overview of its interesting properties.

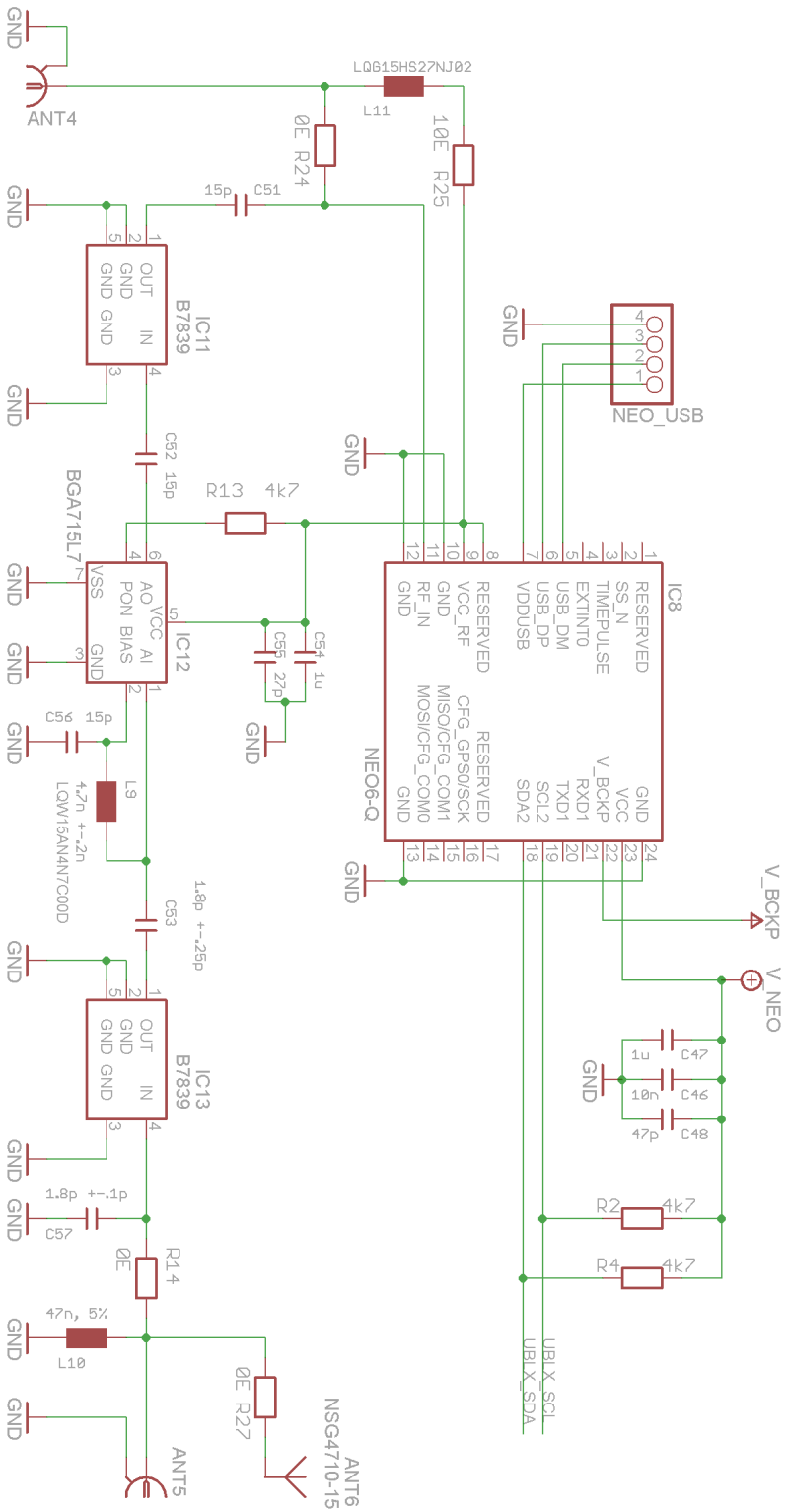

Figure 3.17: Schematic of the GPS module

The NEO-6Q is connected to the GSM module via the DDC port (UBLX_SCL and UBLX_-SDA). Both interface lines are pulled high with the obligatory 4.7kΩ pull-up resistors. To connect a computer to the GPS module (for testing purposes), the USB lines USB_DM, USB_DP and VDDUSB are connected to a 1x4 pinhead. If USB is not used, VDDUSB has to be connected to ground (according to [48]). The voltage at VDDUSB must not exceed 3.6V, so an external LDO has to be applied, if one wants to use this interface. Generation of the backup voltage applied to the V_BCKP pin is discussed in the following subsection *Backup Voltage for GSM and GPS Module*.

Power Supply Voltage Range	2.7V to 3.6V
Max Supply Current	67mA
Supply voltage USB	3.0V to 3.6V
Backup battery voltage	1.4V to 3.6V
Backup battery current	22μA
Size (50-Pin)	16.0x12.2mm^2
UART, DDC (I^2C compliant), SPI, USB	
TCXO (Kickstart for better signal acquisition)	
RTC Crystal	
External Interrupt/Wakeup	

Table 3.12: Main parameters of the GPS module NEO-6Q

To try different antenna layouts, two antenna paths are implemented. A SMA jack ANT4 is connected via a 0Ω resistor to the RF_IN pin and represents the first path. At this SMA jack an external active GPS antenna can be connected to the module and is then powered over the inductor L11 and resistor R25 which are connected to the RF supply voltage pin VCC_RF of the GPS module. The second antenna path is described in [48] as a "passive antenna design for best performance and increased immunity to jammers such as GSM". It consists of a SAW-LNA-SAW structure with the SAW filters B7839 of EPCOS and infineon's low-noise amplifier BGA715L7. These devices and peripherals (with the according values) are taken from the C16 telematics reference design of u-blox [49]. After the SAW-LNA-SAW chain there is a SMA jack ANT5 and a ceramic SMD patch antenna ANT-NSG4710-15 of Round Solutions with 15x15mm^2 patch size, that can be disconnected with the 0Ω resistor R14. PCB layout considerations are discussed in section 3.3.3.

The GPS module is power with 3.0V generated by TI's TPS79930 LDO voltage regulator (see figure 3.18), whose enable input pin EN is connected to LEON's GPIO2 pin (GPIO2_NEO_-EN). Whenever GPS is enabled by the specific AT command, the GPIO2 pin is automatically set high, the voltage regulator starts operating and powers the GPS module. The TPS79930 (see [50] for datasheet) has been selected to meet the power requirements of NEO-6Q.

Backup Voltage for GSM and GPS Module

Both, LEON-G100 and NEO-6Q, have internal components, that require an external applied backup voltage, if the devices are not powered. The GSM module requires a backup source

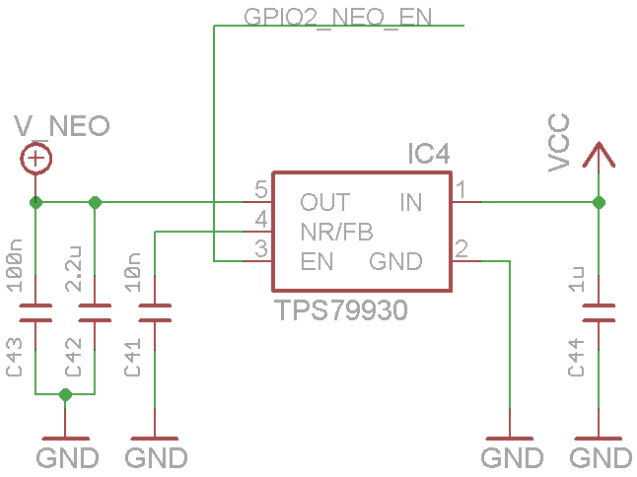

Figure 3.18: Generation of the power supply for the GPS module

of 1.0V to 2.25V with a current consumption of 2.0μA to power its internal RTC. If the module is connected to a voltage source at the VCC pin, a 2.0V voltage is generated and output at the V_BCKP pin. The GPS module needs a backup voltage of 1.4V to 3.6V and sinks 22μA (for the battery backup RAM and the internal RTC).

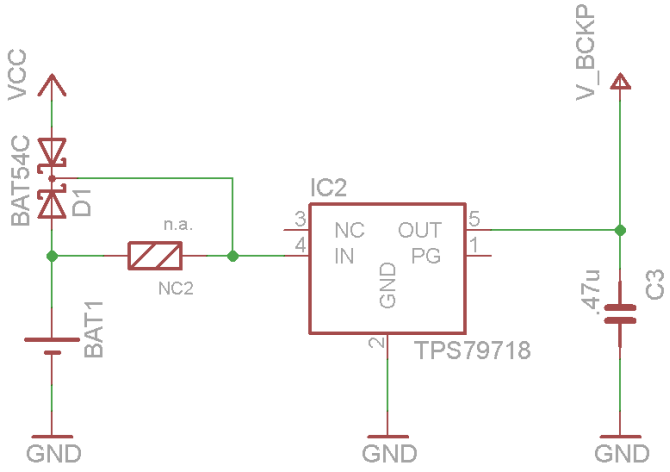

Figure 3.19: Generating backup voltage for GSM and GPS module

Figure 3.19 shows the generation of the backup voltage. The V_BCKP line is directly connected to both modules. If no battery is connected to the Repeater hardware, a LDO voltage regulator TPS79718 generates 1.8V from a backup battery BAT1 (2.0V to 5.5V) connected to its input pin IN. The LDO's output voltage of 1.8V meets the required backup voltage range of both modules. With the first Schottky diode in D1 (upper diode) it is possible to generate the backup voltage using the Repeater's main supply voltage (3.3V). This is useful, if the LEON-G200 is disconnected from the VCC line (e.g. with a high-side

switch) and cannot generate the 2.0V backup voltage. The second diode in D1 (lower diode) is implemented to avoid charging the backup battery. If one wants to use a rechargeable battery, a 0Ω resistor has to be applied to the part NC1.

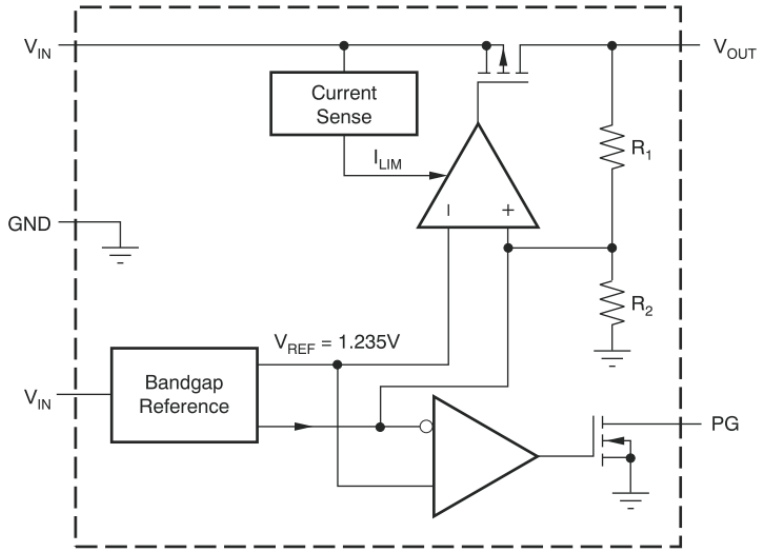

Figure 3.20: Functional block diagram of the internal components of the TPS79718 [51]

If a battery is connected to the Repeater, the GSM module LEON provides a voltage of 2.0V on the V_BCKP line for the GPS module. A higher voltage (2.0V compared to the output voltage of the TPS79718 of 1.8V) does not affect the voltage regulator due to its internal circuit (see figure 3.20). The output voltage at V_{OUT} is supplied via a voltage divider to the internal comparator. The divided voltage is then compared to an internal reference. If the output voltage is too high, the comparator output will exceed its positive supply voltage. Therefore, the gate-to-source voltage U_{GS} increases to 0V and the p-channel MOSFET is turned off.

3.3.2 Firmware

The Repeater is used to communicate with the Sensor within defined intervals and send SMS or emails on specific events. It is also a battery powered device, and therefore low power consumption is requested again. Like in the Sensor firmware, the microcontroller is set to low-power mode as long as possible. The Repeater implements the basic functionality of the daemon running on the UNIX based system in the smaXtec Base Station. This includes only the commands for flash and data readouts. On the Repeater no periodical measurements are performed. Because of its access to the Internet, the Repeater could also be used to fetch all data of a Sensor and transfer it to a smaXtec data server. The basic functions to implement this feature (HTTP POST of data and files, FTP upload) are already implemented and have been tested.

Main State Machine

For configuration purposes, the Repeater has the same functionality as the Sensor (see the states **READY** and **SELECTED**). Therefore, the message interpreter is identical to the one implemented in the Sensor firmware described in section 3.2.2. A chart of the state machine is given in figure 3.21.

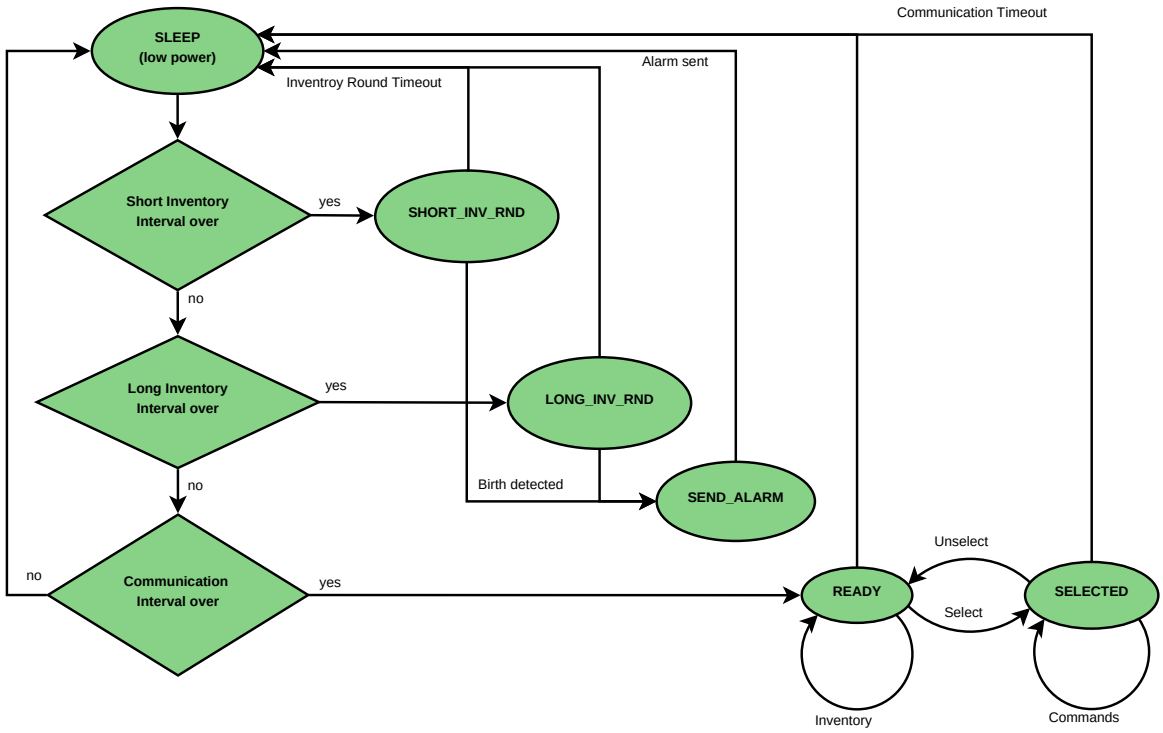

Figure 3.21: State chart of the Repeater firmware

There are three new states introduced for the Repeater: **SHORT_INV_RND**, **LONG_INV_RND** and **SEND_ALARM**. The two inventory round states have the same functionality but differ in duration. A long inventory round (**LONG_INV_RND**) is used to fetch and read data of all sensors applied to an animal and upload it to the Internet. The calving detection itself is planned to be done inside the Sensor firmware. The Sensor should then inform the Repeater as soon as a calving event has been detected. This is done by setting the Sensor into continuous receiving mode (by reducing its communication interval), when an upcoming event has been detected. The Repeater will then fetch the Sensor and read its data in the next short inventory round (**SHORT_INV_RND**). A short inventory round lasts only for a few seconds but is started more frequently. When the Repeater has read the data, the Sensor resets its communication interval to the default value (see section 3.2.2). Table 3.13 shows the currently used time intervals and durations for the state changes.

If the Repeater is used to read and upload data to the Internet, the long inventory should last at least 2x $T_{CommunicationInterval}$ of the Sensor with the longest communication interval

Description	Value
$T_{CommunicationInterval}$	15sec[1]
$T_{CommunicationTimeout}$	3000msec
$T_{longInventoryRoundInterval}$	21600sec ($\widehat{=}$6h)
$T_{longInventoryRoundDuration}$	600sec ($\widehat{=}$10min)
$T_{shortInventoryRoundInterval}$	300sec ($\widehat{=}$5min)
$T_{shortInventoryRoundDuration}$	5sec

[1] only for testing purposes. In operation this value will be around 300sec ($\widehat{=}$5min).

Table 3.13: Intervals and timeouts for the main state machine

(see [40] for detailed information). Transmitting and listening for incoming packages over such a long period is very power consuming (20mA to 25mA during TX and RX mode), so the long inventory round should be done very rarely (e.g. four times a day). This results in bad data actuality, so a trade-off between timeliness of data and Repeater lifetime has to be found. A second approach would be to synchronize data exchange between Sensor and Repeater via the time of day available in the RTC.

If a calving event has been read by the Repeater, the **SEND_ALARM** state is entered. The Repeater powers on the GSM and GPS module and starts forwarding the alarm to the human supervisor via SMS or email. A detailed description is given in the following subsection *Send Alarm*.

Inventory Round

An inventory round for data readout (for calving detection) is shown in the state chart in figure 3.22. The start of an inventory round is triggered by a TimerA timeout within the given (short and long) interval and with the given duration specified in the configuration. Every 300ms an *AnimalInventory* (see section 3.2.2 for definition) is sent via the RF interface. If a Sensor replies including the correct *animalId*, a *Select* command is sent to the Sensor. If the Sensor configuration received by the *ReadFlash* command contains a correct device type (here the type Calving Detector), the amount of data available is fetched (*QueryData*) and the last entry is read. If it is an incorrect device type or no data is available, the *Quiet* command is sent to the Sensor, so that it does not answer anymore in this inventory round. If a command failed, the Sensor is set back to ready state (*Unselect*) and data reading is tried again with the next *AnimalInventory*. If measurements have successfully been read and analyzing the data detects a calving event, the Repeater enters the **SEND_ALARM** state in the main state machine. If no event has been detected, the inventory round lasts until its duration is over, returns to the main state machine and enters the sleep state.

Send Alarm

Transmitting the alarm to the supervisor is all done by sending AT commands to the GSM module LEON-G200. All available AT commands are described in [52]. A chart of the

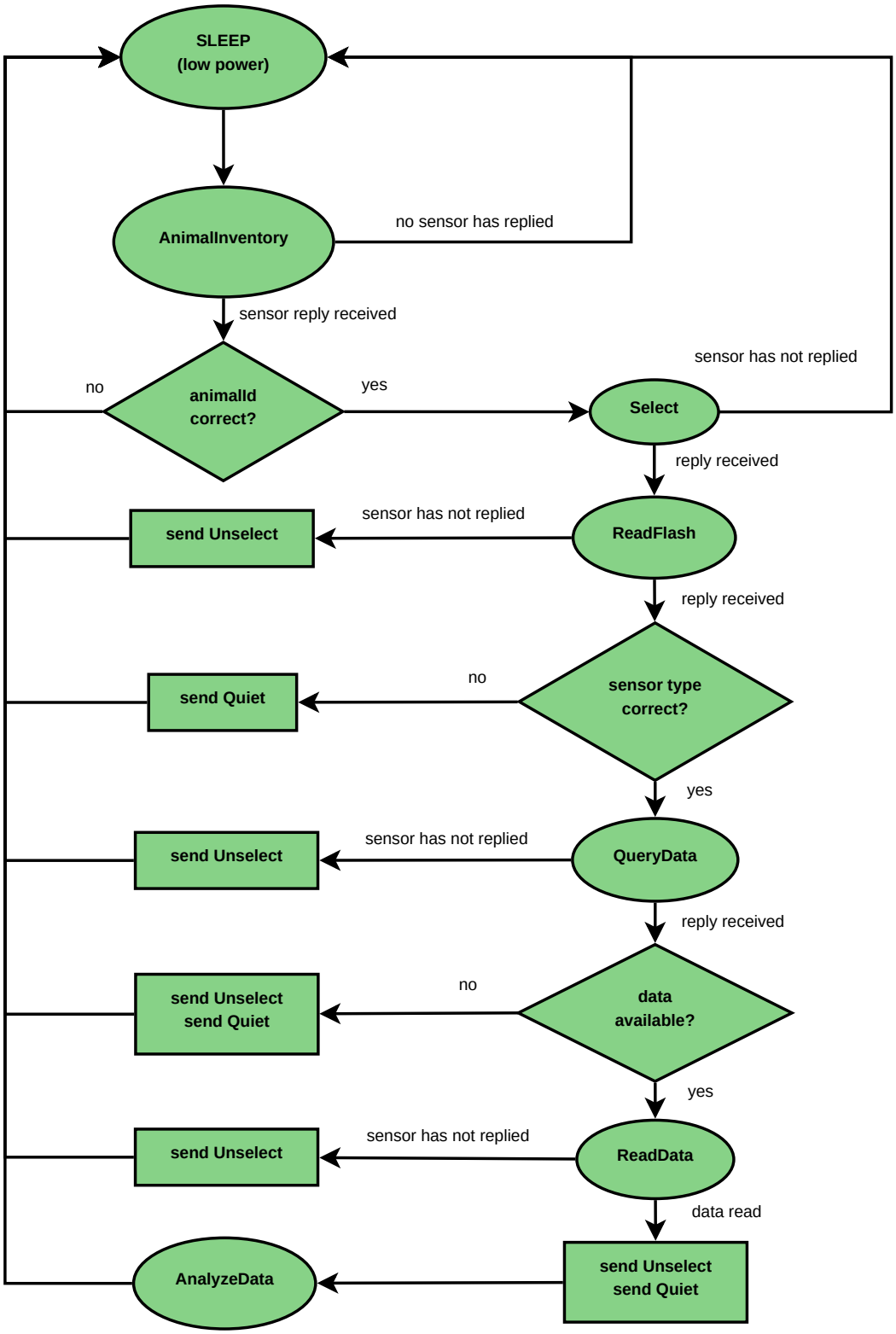

Figure 3.22: State chart of the inventory round for fetching Sensor data

command chain for transmitting the alert is shown in figure 3.23 and table 3.14 gives a summary of important AT commands.

AT Command	**Description**
`ATE0\r\n`	local echo off
`AT&K0`	disable hardware flow control
`AT+CSQ\r\n`	returns signal quality and bit error rate
`AT+CIND?\r\n`	returns status of the data module (battery, network status, SMS, GPRS, etc.)
`AT+UGAOF=...\r\n`	AssistNow offline configuration
`AT+UGAOP=...\r\n`	AssistNow online configuration
`AT+UGPS=...\r\n`	GPS control (power on/off, with/without aiding)
`AT+ULSTFILE=0\r\n`	returns the file list of LEON
`AT+UDELFILE=...\r\n`	deletes the file with the given name
`AT+UPSV=2\r\n`	disable hardware flow control
`AT+UPSD=...\r\n`	GPRS initialization
`AT+UPSDA=...\r\n`	GPRS action (reset, load, store, activate, deactivate)
`AT+USMTP=...\r\n`	SMTP settings
`AT+USMTPM=...\r\n`	SMTP mail control
`AT+USMTPC=...\r\n`	SMTP control (connect, send mail, quit)
`AT+UGUBX=...\r\n`	send u-blox protocol messages to the GPS module and receives the answer
`AT+CPWROFF\r\n`	switch off the GSM module

Table 3.14: Summary of important AT commands [52]

The startup of LEON-G200 is done by forcing the RESET and PWR_ON pin to ground for 50ms (min 5ms are required). Applying a low level to the RESET pin is not required, but if the device is running for any reason, it is reset and a clean startup can be performed. After pulling both lines to high again, the CC430 waits for 1500ms until the GSM device has finished the power on sequence (the startup phase of LEON-G200 is shown in figure 3.24). After the startup, a basic initialization is done. For easier reply-parsing and less data transfer, the local echo is turned off. To enable the power save mode of LEON the hardware flow control (via RTS and CTS) is disabled. The next step is to setup GPRS (enter provider APN, username, password) and SMTP (enter server, username, password and authentication type).

Because both modules are connected via the DDC interface, the NEO-6Q GPS module can be started with AT commands sent to the LEON-G200 GSM module and aiding information can be applied to the GPS module. This feature of u-blox is called AssistNow. With aiding information GPS fixes in *cold start* can be achieved much faster (see TTFF list in table 3.15, where Time-to-first-fix is the time needed by the GPS receiver to get its first correct position). By starting the GPS module in AssistNow offline mode (with enabled GPRS connection), a differential almanac correction data file is downloaded from the u-blox server. When starting with AssistNow offline mode (after an undefined off-period of the GPS module), one should

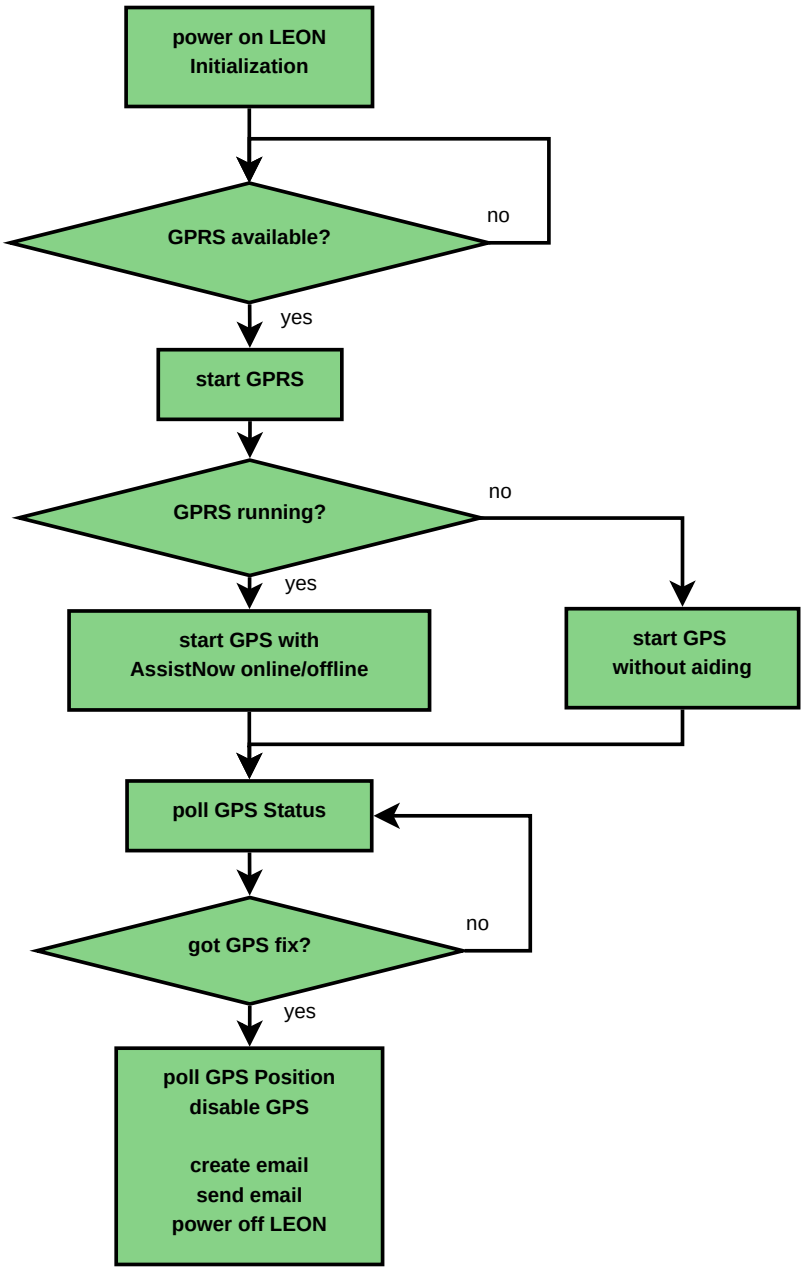

Figure 3.23: Simplified state chart of the send alarm command chain for the u-blox devices

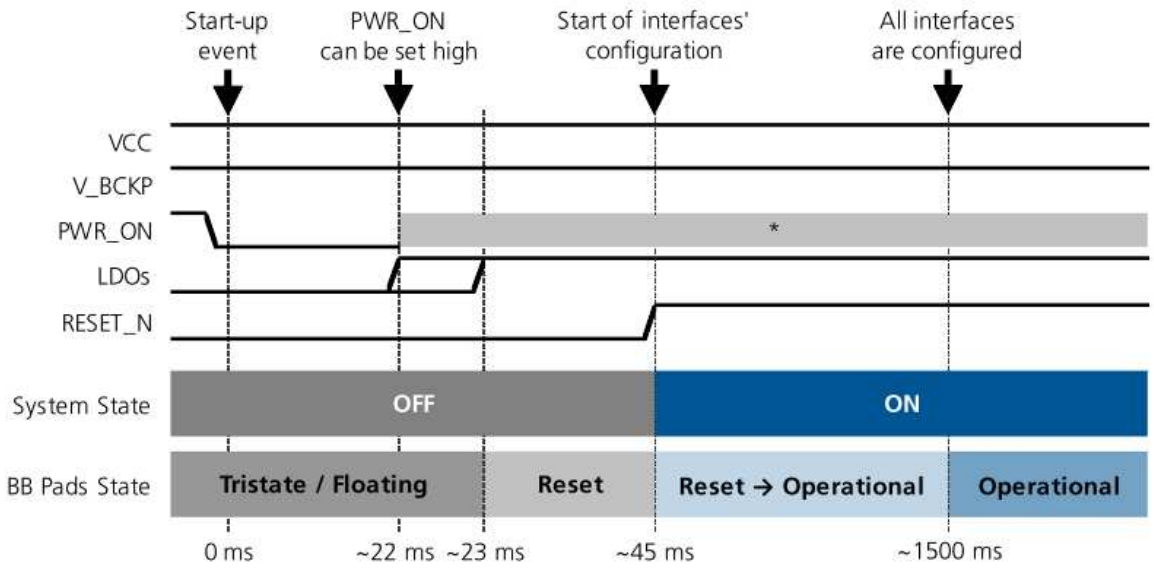

Figure 3.24: Power on sequence description (* - the PWR_ON signal state is not relevant during this phase) [45]

Time-To-First-Fix (TTFF)		
Cold start	29sec	Receiver has no information on the last position (e.g. time, velocity, frequency etc.) at startup. Therefore, the receiver must search the full time and frequency space and all possible satellite numbers.
Warm start	29sec	Receiver has approximate information on time, position and coarse satellite position data (Almanac). The receiver basically needs to download ephemeris until it can calculate position- and velocity data. As the ephemeris data usually is outdated after 4 hours, the receiver will typically start with a warm start, if it has been powered down for more than 4 hours.
Hot start	$<$ 1sec	The receiver has been powered down only for a short time (4 hours or less), so that its ephemeris is still valid. Since the receiver does not need to download ephemeris again, this is the fastest startup method.
Aided starts	$<$ 1sec	Aiding information (almanac, position, time, ephemeris, almanac, health and ionospheric parameters) is uploaded to the GPS receiver at start-up. Therefore, the receiver can acquire a fix faster much.

Table 3.15: Time-To-First-Fix of NEO-6Q (for all satellites at -130 dBm) [44, 53]

check first, if a valid almanac file is on the flash file system or delete all available **.alp* files, to ensure correct almanac data is used. u-blox provides files with validity from 1 to 14 days. When starting in AssistNow online mode, assistance data is downloaded from the u-blox AssistNow Online Server [30].

After the GPS has been started, communication with the NEO-6Q is available with an AT command sent to LEON (`AT+UGUBX`) that forwards the given message via DDC. NEO supports four protocols namely NMEA, UBX, RTCM and RAW. The NEMA protocol transfers data in ASCII format, what makes it easy to read but difficult to parse within firmware. Therefore, the u-blox proprietary UBX protocol is used, where 8bit binary data is transmitted. The format of a UBX packet is shown in figure 3.25. *SYNC CHAR 1* ($0xB5$) and *SYNC CHAR 2* ($0x62$) indicate the start of a UBX message. With *CLASS* (message subset) and *ID* (message identifier) a certain message is defined. The two byte *LENGTH* field specifies the length of the payload. After the payload, there are two bytes of checksum, which are calculated over the bytes marked with green hatching (Class, Id, Length and Payload) using the following piece of pseudocode [53].

```
CK_A = CK_B = 0
For(I = 0; I < N; I++)
{
    CK_A = CK_A + Buffer[I]
    CK_B = CK_B + CK_A
}
```

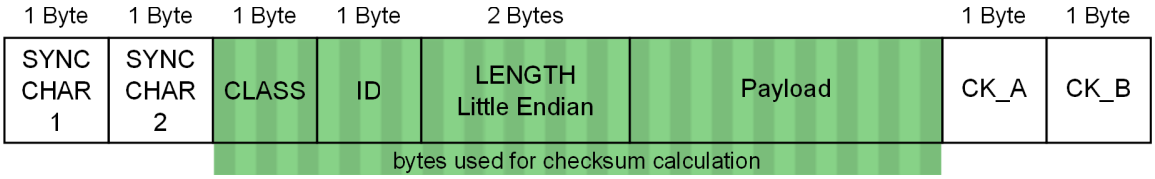

Figure 3.25: Format of an u-blox proprietary UBX packet [53]

Polling for a specific message is done by just sending the requested message (Class and Id) to the module with no payload (LENGTH = 0). Therefore, a message request has a length of 8 bytes. UBX messages replied by the GPS module can be parsed very easily by just performing a checksum calculation and simply casting the data into a data struct according to the message class and id. Using the NMEA standard would cause an enormous effort in string parsing.

After enabling the GPS module, the Receiver Navigation Status (*NAV-STATUS*) is requested to check, if a GPS position has successfully been calculated. The message is polled in a loop until a GPS fix has been reached. Afterwards the Geodetic Position Solution (*NAV-POSLLH*) is polled containing latitude, longitude, height and horizontal + vertial accuracy estimates for the GPS position. These information is then packed into an email and sent to the supervisor. If all actions have succeeded, both modules are powered down by sending `AT+UGPS=0` and `AT+CPWROFF` to the LEON-G200. The description of the command chain is

kept very simple. Every command can return an error code that has to be considered and different actions have to be performed on different errors.

Memory, RTC, Battery Monitoring, Accelerometer

Battery monitoring works exactly the same way as in the Sensor, it differs only in the port configuration. RTC, memory and acceleromter have already been discussed in the Sensor firmware in section 3.2.2. The only difference to the Sensor is that SPI and I^2C bus share the same interface on the CC430F5137. So before starting a communication with any device, the correct interface has to be initialized (`i2cInit`, `spiInit`).

Configuration

The Repeater configuration again has to look the same as the smaXtec pH Bolus config, to be able to use the smaXtec admin tool. This leads to some dummy values in the Repeater's config. Table 3.16 list the main config parameters or the Repeater.

name	**bytes**	**description**
channel_nr	1	RF channel number (see CC430 datasheet [33])
sensorType	1	this will be used in future to distinguish between different device types (e.g. pH Bolus, Calving Detector, Heat Detector, Repeater)
serial_nr	8	unique sensor identifier
animal_id	16	each animal has its own ID
longInventoryRoundInterval	2	long inventory round interval in sec
longInventoryRoundDuration	2	duration of a long inventory round in sec
shortInventoryRoundInterval	2	interval of a short inventory round in sec
shortInventoryRoundDuration	2	duration of a short inventory round in sec

Table 3.16: Main Repeater configuration parameters

3.3.3 PCB Layout for Antennas

The Repeater has three different RF interfaces: GSM, GPS and a 433MHz interface. For all strip lines to the antennas (or the SMA jacks) a 50Ω output resistance is required. To calculate the geometric dimensions for the strip lines, *AppCAD* from Agilent Technologies has been used. Figure 3.26 shows a screenshot of the calculation for the coplanar waveguide with groundplane. The necessary parameters for calculation are listed in the following table.

Parameter	value	description
H	1000μm	given by PCB supplier PIU-PRINTEX for material FR4 - 104
T	35μm to 43μm	
ϵ_r	4	
G	200μm	limited to 200μm by CadSoft EAGLE PCB Design Software
W		adapted

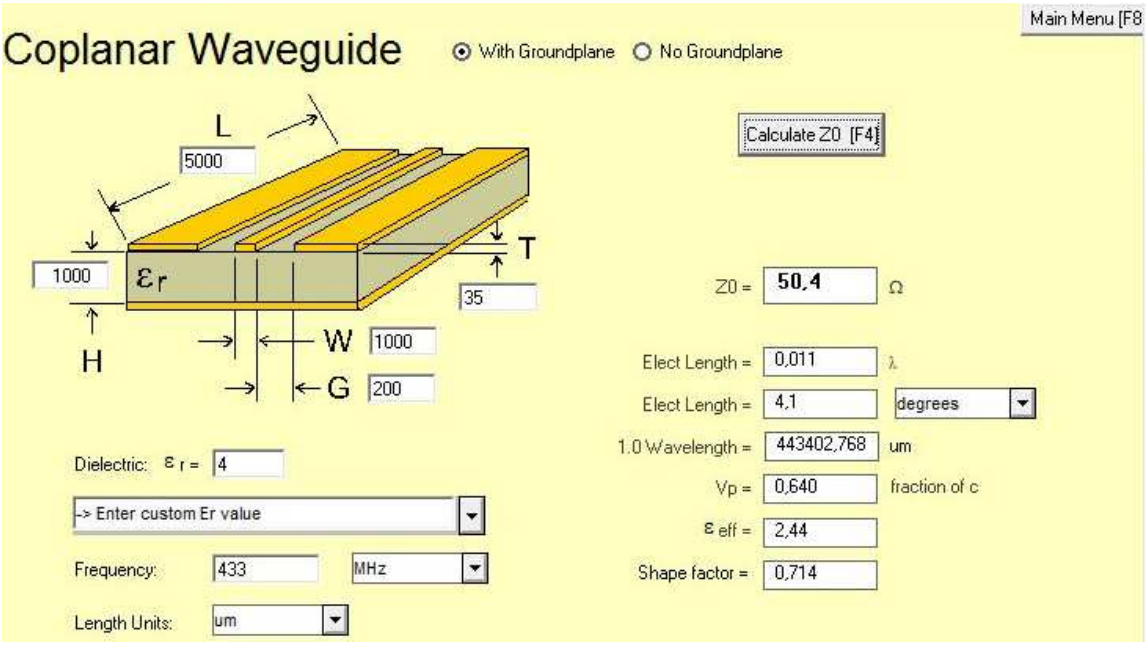

Figure 3.26: Results of calculating the impedance of the grounded coplanar waveguide with *AppCAD* of Agilent Technologies.

Frequency and length of the line L do not affect the calculated impedance $Z0$. With the given parameters, the line width W has then been adapted to get an impedance of 50Ω. A value of $W = 1000\mu$m results in the best impedance over the range of copper height from $T = 35\mu$m to 43μm ($Z0 = 50.4\Omega$ to 49.6Ω). A higher value for the gap $G > 200\mu$m results in a higher impedance $Z0$. Therefore, a line width of $W = 1$mm with a gap to the ground plane of 0.2mm is used for the strip lines to the antennas or SMA jacks.

The following figures 3.27, 3.28 and 3.29 show the layout of the three antenna paths. The 433MHz interface uses the same balun as already discussed in section 3.2.3. The GSM module (figure 3.28) does not need an external matching circuit. The active antenna path (blue) for the GPS module (figure 3.29) does not need a matching circuit either. Therefore, antennas can be connected directly to the modules. The yellow path shows the SAW-LNA-SAW chain close to the module and is connected to a SMA jack and the patch antenna via the 1mm wide strip line. Both antenna paths are fed into the RF_IN pin (green).

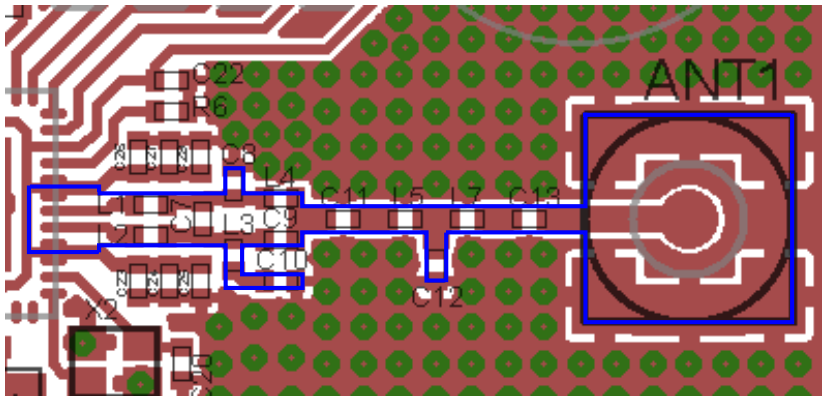

Figure 3.27: The blue marked path shows the converter from differential to single ended load and the antenna matching circuit (as recommended by Texas Instruments in [33]) and the SMA jack for an external 433MHz antenna.

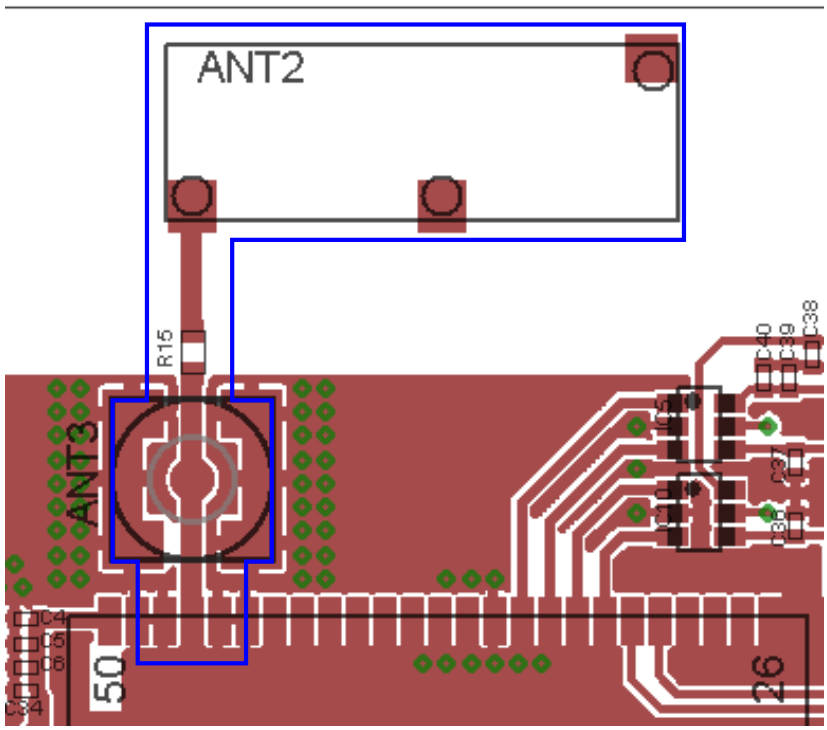

Figure 3.28: Layout for the on-board GSM antenna with the SMA jack connected to the ANT pin of LEON-G200 (marked in blue).

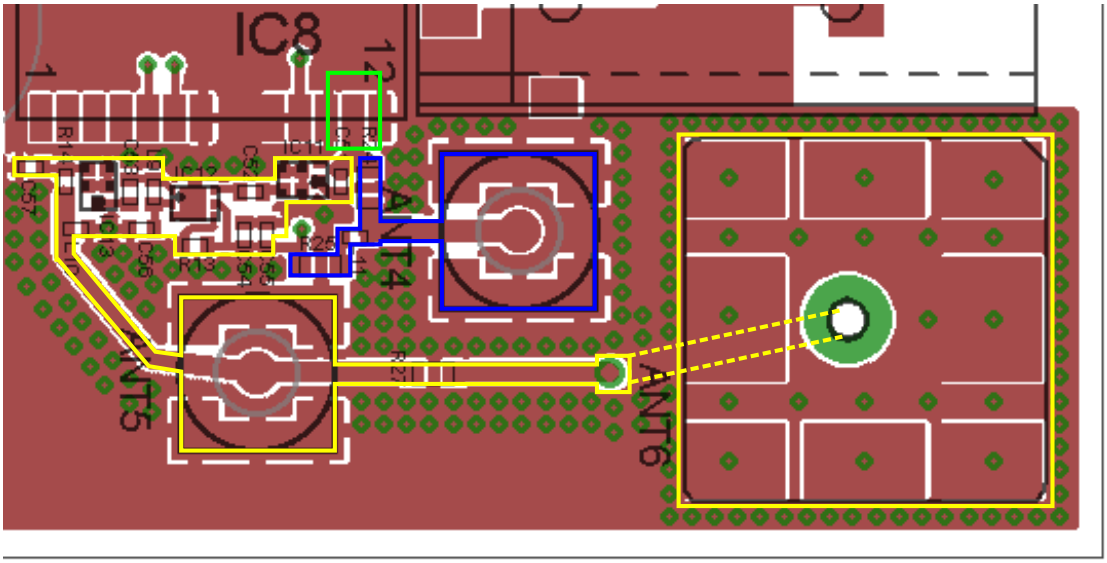

Figure 3.29: Layout for the two antenna paths for external active antennas (blue) and for the on-board GPS antenna with the SAW-LNA-SAW chain (yellow). Both paths are connected to the RF_IN pin of NEO-6Q (green).

4 Evaluation

This chapter deals with the evaluation of the used measurement devices accelerometer, Pt1000 and ADC for temperature reading, and GPS + GSM modules. The last section discusses the signal strength at the 433MHz RF interface measured in the Sensor - Repeater system applied to an animal.

4.1 Movement and Freefall

The accelerometer for movement recording and freefall detection has been tested in three different cases. The first two tests described in the following subsections show the results of motion recording and the third test ensures that freefall events can be detected.

4.1.1 Movement during Sports Activities

The accelerometer and its movement recording has been tested during sports activities. Two Sensors have been used to record the movement over 9 hours of activity. Figure 4.1 shows the result of the test. The upper graph shows the raw movement index whereas the lower graph represents the low-pass filtered data with a cut-off frequency of $f_c = 2.5$Hz. The figure displays the activity from 6:00am to 3:00pm. The test person has recorded the start of sports activity at 6:45am, and pauses at 9:30am to 9:45am, 11:00am to 12:00am and 1:00pm to 1:45pm. The end has been stated with 2:30pm.

Comparing these information with the graphs shown in figure 4.1 with three periods of inactivity (resting) from 9:30am to 9:50am, 11:00am to 12:00am and from 1:00pm to 1:40pm corresponds to the data recorded by the test person. The higher motion index during the afternoon has also been confirmed by the test person.

A detailed view of the recorded movement index between 8:00am and 9:00am is given in figure 4.2. A close relation between both curves can be detected with a slight offset of time (about 2minutes). This offset has two major reasons. Both Sensors have been started at different times. Therefore, their measurements are done over different periods of time. Setting the time for the RTC also causes errors, because with the *Set Time* command, performed by the admin tool, the current time is only set with hours and minutes. Seconds are always set to zero. These facts do not affect the correctness of data. It is less important to have an exact matching between data and time, but to have a recorded value that is equivalent to the intensity of movement.

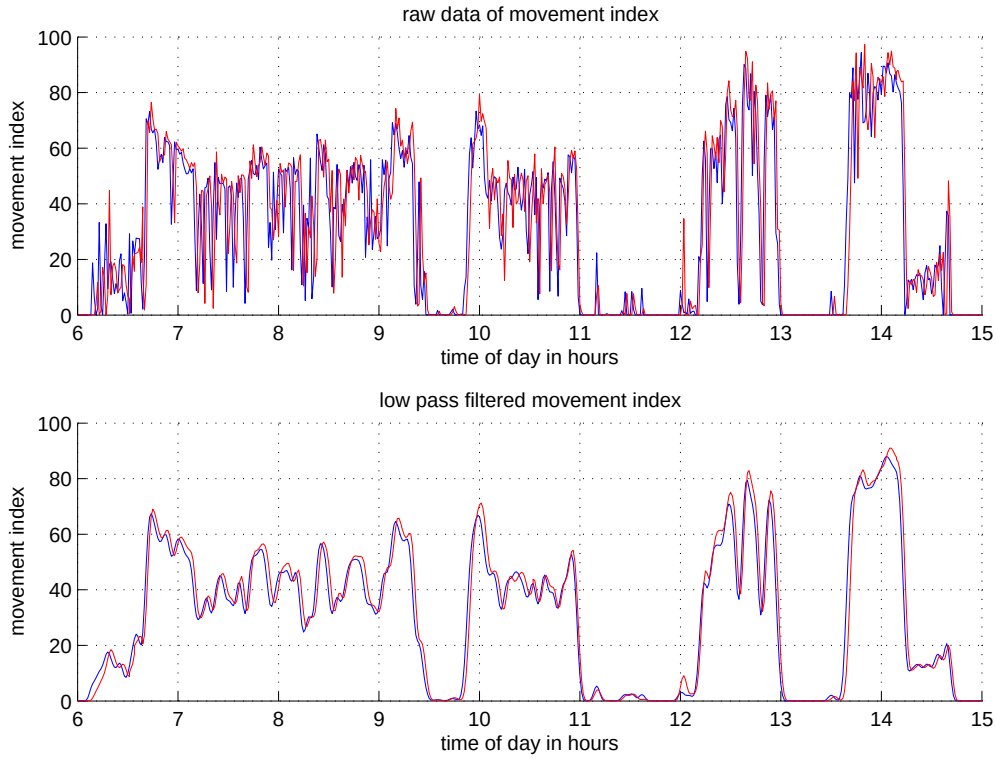

Figure 4.1: Movement index over the time of day during sports activities. The upper graph shows the raw data, the lower graph shows a low-pass filtered dataset with a cut-off frequency of $f_c = 2.5$Hz.

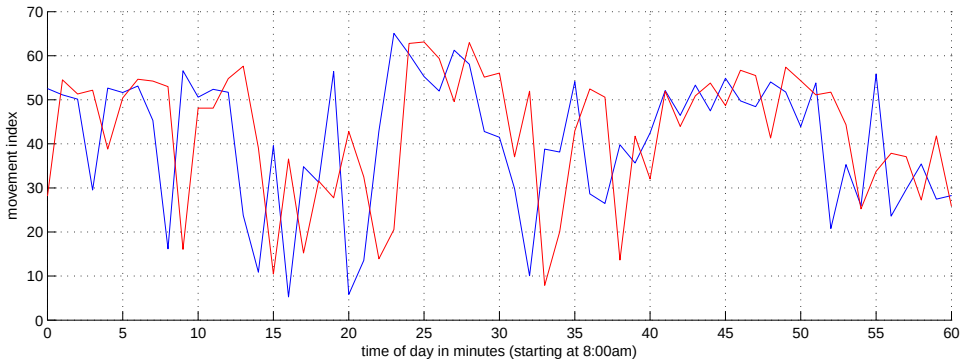

Figure 4.2: Detailed view of the movement index over one hour

4.1.2 Movement of Cattle

A second test has been performed by mounting the Sensor on the collar of a cow (see figure 4.3). This has been done at around 9:45am and at 15:45pm the Sensor has been unmounted again. The movement data (figure 4.4) corresponds to the resting of the cow recorded from 11:00am to 11:30am and 1:15pm to 1:45pm. Recording the reference data has been done visually in steps of 15min ±3min. Between 12:00am and 1:00pm no reference data has been taken.

Figure 4.3: Mounting of movement Sensor onto the cows collar

The low-pass filtered data is useful for comparison of movement data of more Sensors on a test person. For heat detection other filters might be more useful. Maybe the peaks in the raw data around 10:30am, 12:00am and 12.45am are of real interest. But the filter and algorithm design can only be done, when reference data is available.

4.1.3 Freefall Detection

Testing the freefall detection has been performed by simply dropping the Sensor from a height of 1m. The Sensor has set itself to continuous receive mode and the admin tool has been able to read its data and having the event detected. Dropping the Sensor from a lower height of 0.5m has not been recognized as an freefall event (due to the calculated threshold described in section 3.2.2).

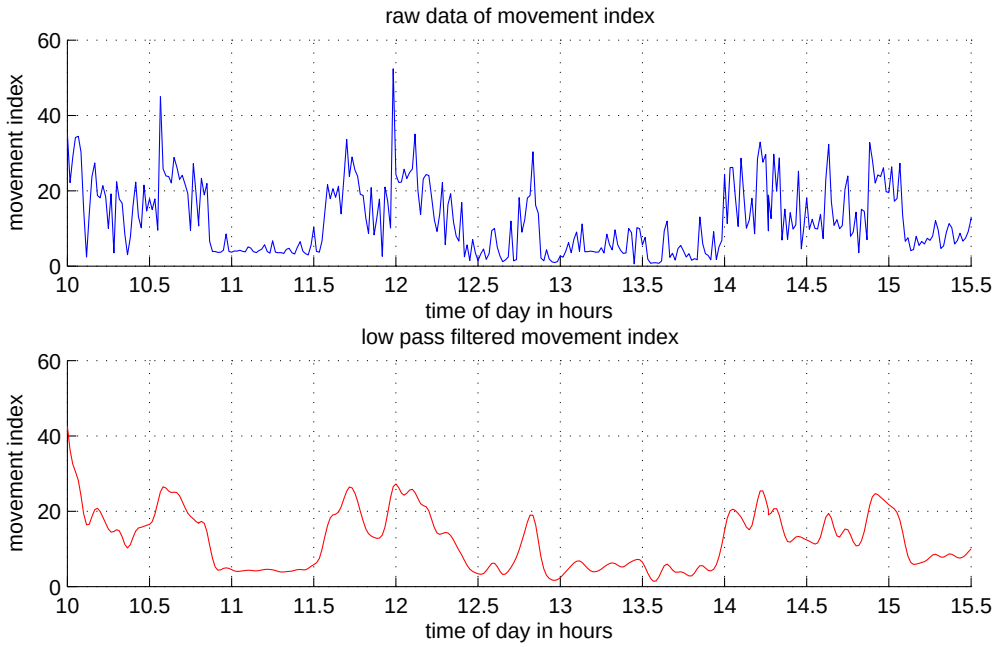

Figure 4.4: Movement index of a cow kept in loose-housing system from 10:00am to 3:30pm. The upper graph shows the raw data, the lower graph shows the low-pass filtered dataset with a cut-off frequency of $f_c = 2.5$Hz.

4.2 Temperature

During sports activities described in the previous section 4.1, also the outdoor temperature has been recorded. The data is shown in figure 4.5 with a relevant range from 6:45am to 2:30pm (as described in section 4.1). From the beginning until 9:30am (first inactivity) and from 10:00am to 11:00am the test person has been moving without being exposed to sunlight in shady and cold fields, whereas the first period of inactivity has been recorded with direct sunlight. During inactivity from 11:00am to 12:00am the Sensor has been situated in a warm but shady area. Afterwards it has been exposed to direct sunlight again. Constant temperature from 1:00pm to 1:30pm comes again from a shady area followed by higher temperature caused by direct sunlight.

Evaluation of the functionality of the temperature measurement has been done using the *RCT basic IKAMAG® safety control*. Figure 4.6 shows the test arrangement with two Sensors on the left with a Pt1000 resistor connected via 30cm of copper wire, a *Fluke True RMS DMM with 80BK Temperature Probe* for temperature reference measurements and the *RCT basic* for controlled heating of the glass container with 1.2l water.

Prior to the evaluation both Sensors have been single-point calibrated with a $1.1\text{k}\Omega \pm 0.1\%$ resistor instead of the Pt1000 ($1.1\text{k}\Omega \mathrel{\widehat{=}} 25.684°\text{C}$) connected with the same length of copper wire. The water has been heated to 25°C and temperature kept constant for some time.

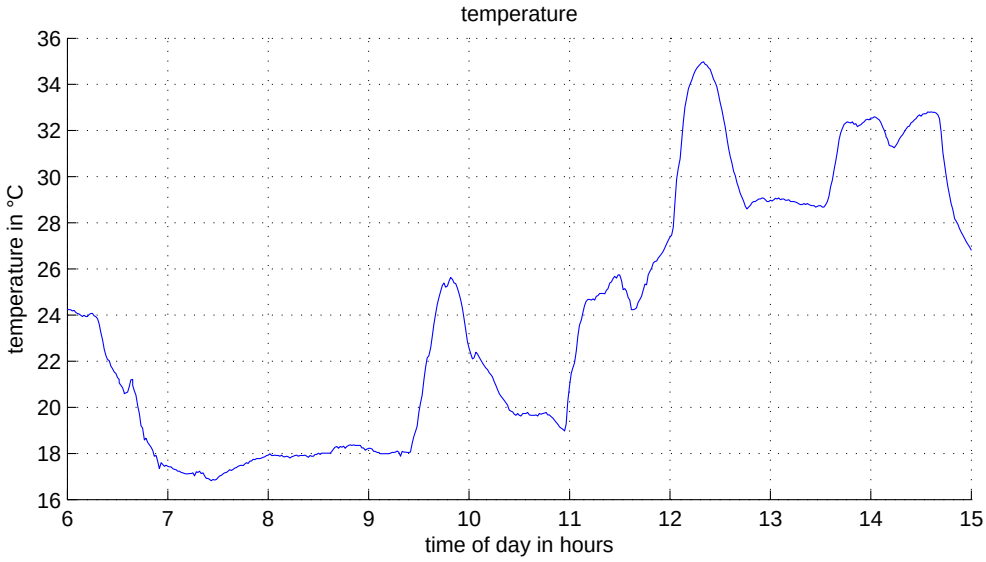

Figure 4.5: Outdoor temperature recorded during sports activities

Figure 4.6: Arrangement for evaluation of temperature measurement with two Sensors (bottom left), Fluke 179 measuring temperature reference (bottom right), and a glass container on the *RCT basic* heating system (center).

Then the heating system has been set to heat up to 36°C. Measurements of both Sensors (blue and green) follow the curve of the reference data (colored magenta).

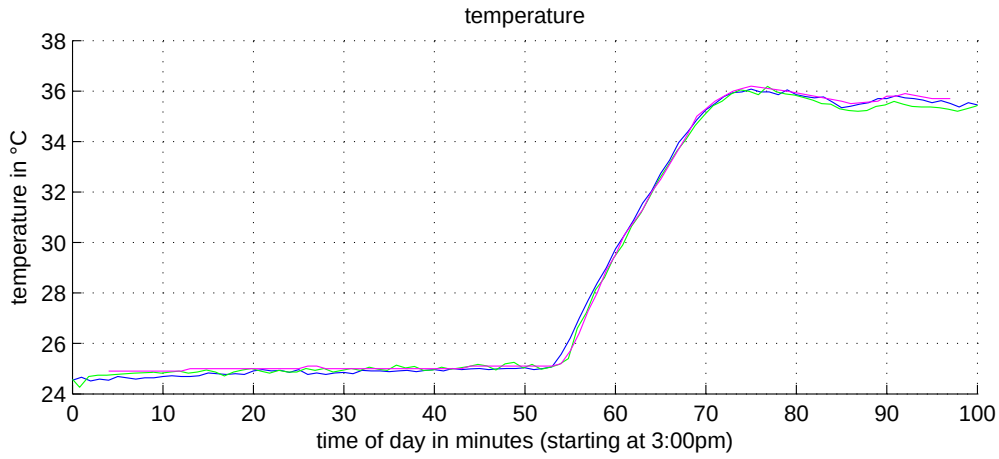

Figure 4.7: Comparison of Sensor temperature (blue and green) with recorded reference (magenta)

4.3 GPS + GSM Modules

As part of the preparation for the evaluation of GPS and GSM module, all different antennas have been tested. The following two subsections describe the antenna tests that have been performed and discuss the results. The last tests proves the correct functionality of both modules.

4.3.1 GSM Antenna and Signal Strength Test

The GSM module LEON-G200 has been tested with the PCB mounted antenna ANT-GXE477 of Round Solutions and with two external antennas, ANT-GNW640 (combined GSM and GPS antenna) of Round Solutions and a GSM antenna supplied by u-blox. The GSM signal quality has been queried with the AT command `AT+CSQ?` and an average over 50 values has been calculated. The reply to this message contains the RSSI, that can be mapped to the "signal" indicator (displayed in mobile devices) according to the following table.

signal indicator	**RSSI value**	**signal strength**
0	< 4 or 99	< -107dBm or unknown
1	< 10	< -93dBm
2	< 16	< -71dBm
3	< 22	< -69dBm
4	< 28	< -57dBm
5	≥ 28	≥ -57dBm

All antennas have been tested indoor under bad signal conditions in the same environment. The results are listed in the following table.

antenna	**signal indicator**	**RSSI value**
ANT-GXE477 (on-board)	3	19.4
Antenna of u-blox (external)	4	22.1
ANT-GNW640 (external)	3	16.7
iPhone 4	3	20
Samsung Galaxy S2	2	14

Comparing these results to the signal quality of mobile phones, equal quality with the on-board antenna and even better quality with the external antennas is gained.

4.3.2 GPS Antenna Test

The GPS input signal has been tested using both antenna paths (see *GSM and GPS Modules* in section 3.3.1). The path for external active GPS antennas can be seen in figure 3.17 via the 0Ω resistor R24 and the SMA connector ANT4 at the end. Supply voltage for the active antenna comes via L11 and R25. When using this path, C51 has to be disconnected from the RF_IN pin of the NEO-6Q module. With the active GPS antennas *ANN-MS-0-005* and *ANT-GNW640* attached to ANT4, GPS has been started using u-blox's AssistNow online A-GPS service and resulted in an cold-start TTFF of 5 to 10 seconds under bad signal conditions (urban indoor environment).

The second path (SAW-LNA-SAW chain with on-board patch antenna ANT-NSG4710-15 of Round Solutions) is enabled by removing resistor R24 and applying C51 again. The SMA jack ANT5 could have be used to connect an external passive GPS antenna, but has not been tested. GPS has again been started with AssistNow online and resulted in a cold-start TTFF of 15 to 20 seconds (same signal conditions as mentioned above). The higher TTFF can come from various problems, but further measurements have to be done to figure them out. Most likely errors are:

- The patch antenna is intended to be mounted on bottom layer. To avoid higher costs in assembly it has been mounted on top layer. Therefore, a longer strip line with a via from top to bottom layer has arisen.
- Antenna mismatch caused by using the matching parts according to the reference design.
- Problems during assembly and soldering of the small ICs in the SAW-LNA-SAW chain.

4.3.3 GSM and GPS Test

Finally, the functionality of both modules has been evaluated using the setup shown in figure 4.8 with the on-board GSM antenna and the external active GPS antenna of u-blox. The Repeater firmware has been setup up to continuously fetch GPS positions and whenever a GPS fix has been achieved, it has connected itself via GPRS to the smaXtec web server and posted the GPS data (containing UTC time, GPS fix (2d or 3d), number of satellites used, latitude, longitude and estimated accuracy) to a PHP script, that has written the data into a text file. This file has been downloaded and analyzed afterwards.

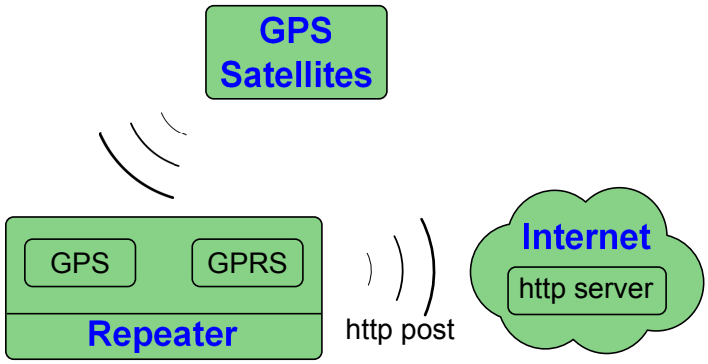

Figure 4.8: Overview of testing GPS and GPRS function of the Repeater

The test has been run in Graz with the Repeater in the backpack. Two tracks with a total of 101 GPS positions have been recorded and evaluated. Figure 4.9 shows the track and all recorded positions as placemarks. The placemarks are colored according to their accuracy estimation in the following way:

accuracy	**color**	**rgb code**
$\leq$ 5m	green	`#00ff00`
$\leq$ 10m	green-yellow	`#c0ff00`
$\leq$ 20m	yellow	`#ffff00`
$\leq$ 40m	orange	`#ff8000`
$>$ 40m	red	`#ff0000`

All placemarks contain additional data for each GPS position, that are date & time, GPS Fix (2 or 3 dimensional), number of satellites used for position calculation and an estimation of position accuracy. The recording has been started and paused indoor (see northern and southern area in figure 4.9), and therefore worse accuracy has arisen there. On the street an accuracy of $\leq$ 10m has been gained. A histogram of the accuracy is given in figure 4.10.

Nearly 40% of the GPS positions have an accuracy $\leq$ 5m and nearly 27% are between 5m an 10m. Therefore, more than a third of all positions recorded in urban area have an inaccuracy of maximum 10m what can be considered as good and sufficient accuracy for our application.

Figure 4.9: The recorded GPS track viewed in Google Earth with additional information

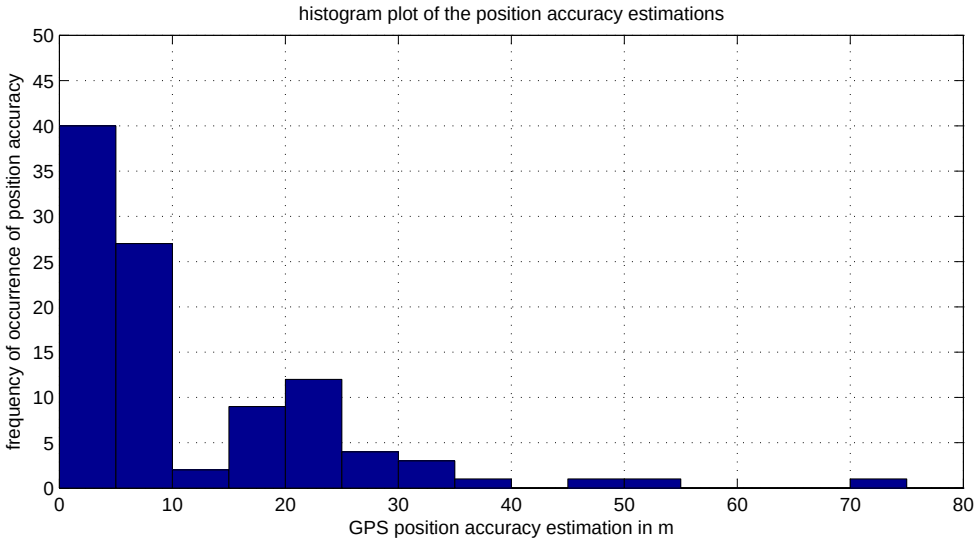

Figure 4.10: Histogram of the GPS accuracy estimations

4.4 433MHz Interface

New developed antennas have been tested, if communication is now possible between the vaginal Sensor and the Repeater at the collar of the cow. Three different antennas have been used: one monopole antenna (see figure 4.11) and two dipole antennas (see figure 4.12 and 4.13). These antennas have prior been developed for a smaXtec application. Figure 4.14 shows the Repeater next to a tied cow and the Sensor inserted into the cow's vagina by the veterinarian Dr. Johann Gasteiner. The Sensor has been aligned that the antenna gears towards the cow's head.

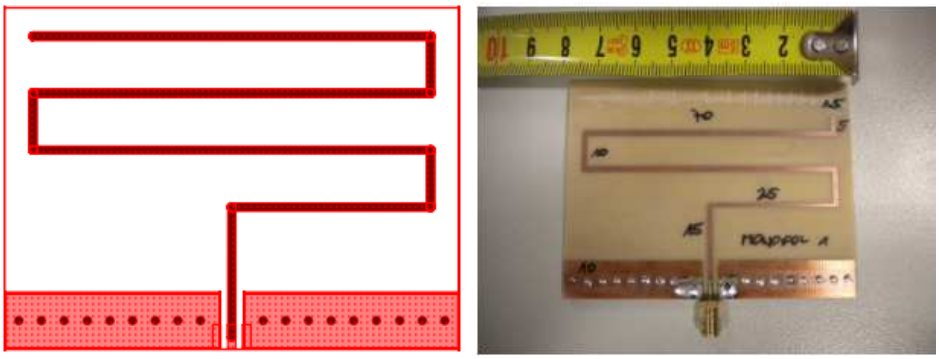

Figure 4.11: 433MHz winding monopole antenna

The Repeater has continuously been broadcasting *Animal Inventory* messages and a Sensor fetching this message has replied to it. Also smaXtec pH Boluses have been in use in the testing area, that have not had the *Animal Inventory* message implemented. Therefore,

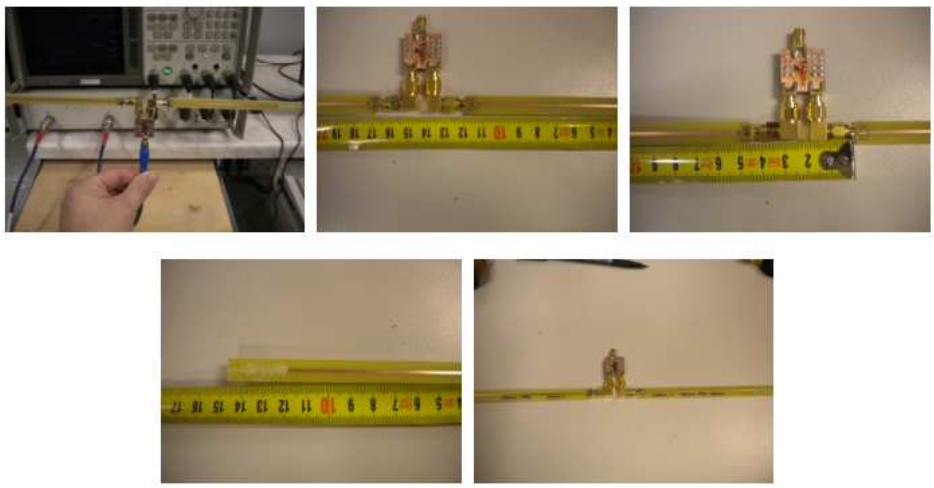

Figure 4.12: 433MHz dipole antenna with straight legs

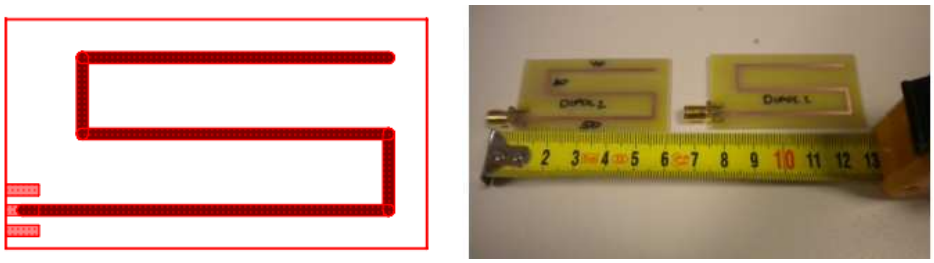

Figure 4.13: 433MHz dipole antenna with winding legs

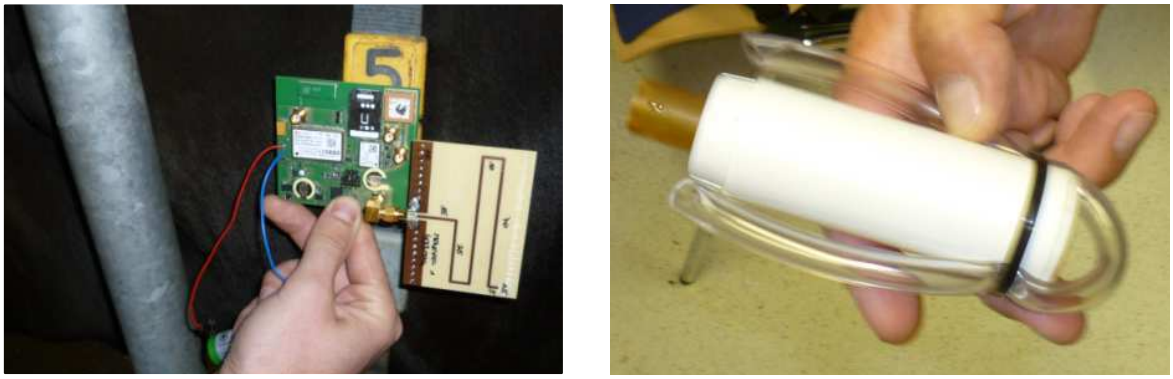

Figure 4.14: Test assembly for the 433MHz RF interface. The Repeater with the monopole antenna connected to the SMA jack (left) and the housing for the vaginal Sensor hardware (right).

they have replied an *Not Implemented* message to the Repeater and these replies have been discarded. The RSSI value of correct replies by the vaginal Sensors have been packed into a new packet (containing date, time, Sensor ID, and RSSI value) and transmitted to the device address 3, that has not been in use. A sniffer hardware, that records all data transmitted on channel 0, has collected all data and sent it via serial interface to a computer. A java tool has picked out the messages sent to device address 3, parsed the content, and output it into a text file. The following table lists some of the collected data.

date and time	**Sensor id**	**signal strength in dBm**
2011 08 10 - 09:16:17	201107000000FF02	-92.0
2011 08 10 - 09:16:31	201107000000FF02	-89.5
2011 08 10 - 09:16:33	201107000000FF02	-97.0
2011 08 10 - 09:16:46	201107000000FF02	-94.0
2011 08 10 - 09:16:49	201107000000FF02	-101.0
2011 08 10 - 09:17:17	201107000000FF02	-90.5

At the beginning, the signal strength around the cow using the monopole antenna has been measured. From the application developed at smaXtec it has been known, that this antenna has good characteristics and it has been easy to apply to the Repeater (see also figure 4.15 on the left). RSSI values have been gathered around the cow at 4 positions and additionally next to the neck and at the back of the neck. Results listed in figure 4.16 show, that the position at the back of the neck gains best signal strength of the Sensor - Repeater system for relevant Repeater positions.

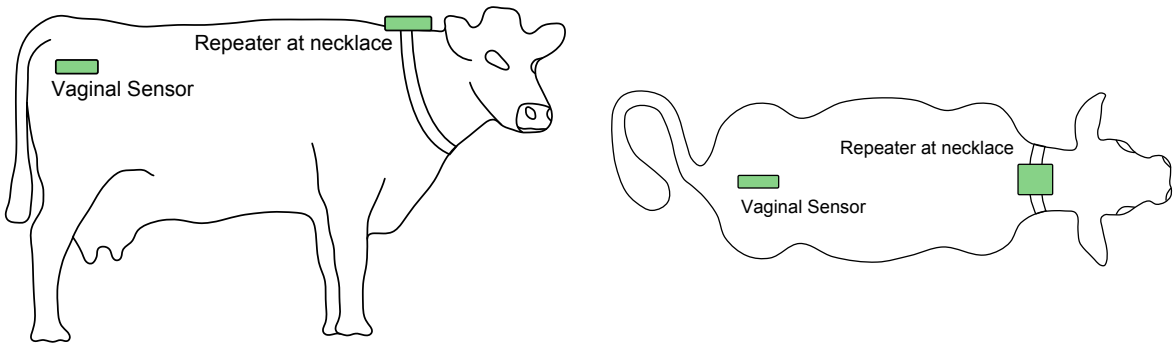

Figure 4.15: Sensor and Repeater position for the 433MHz RF interface test

With this information, the test of all three antennas has been started. The Repeater with each antenna has been placed at the back of the neck (see figure 4.15) with the antenna gearing towards the cow's head and tail. Having the antennas aligned along the backbone has shown very bad results (hardly any data could have been fetched). Therefore, this alignment is not further mentioned. The results are listed in the following table.

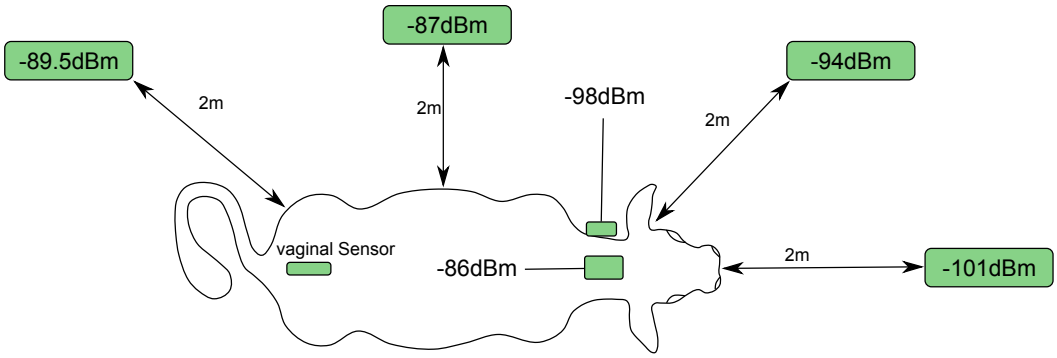

Figure 4.16: RSSI measurement using the monopole antenna. The measured signal strength is indicated at each position.

antenna	**direction**	**signal strength in dBm**
monopole antenna	head	−93.5
	tail	−85.5
dipole antenna with straight legs	head	−94.0
	tail	−90.5
winding dipole antenna	head	−97.5
	tail	−95.0

The test shows, that using the monopole antenna gearing towards the tail gains best signal strength of −85.5dBm in the Sensor - Repeater system, it also needs less space compared to the dipole antennas, and therefore it is the best choice for the Repeater hardware.

5 Conclusion and Outlook

In this thesis a wireless system consisting of a single Sensor for both, heat and calving detection, and a Repeater hardware has been developed. The system integrates temperature and accelerometer measurements into the Sensor for detecting signs of parturition and peak estrus. The Repeater is intended to be used on cows in the late stages of pregnancy and out at pasture. It serves as a relay device forwarding the calving alarms reported by the Sensor device to the stockman via GSM or GPRS. In addition an accurate position of the cow is acquired via GPS and included into the alarm message.

Due to the available interfaces on the Sensor hardware (I^2C, SPI, ADC and RF) and the low power consumption of the complete hardware, it enables an easy integration of different types of sensor chips, and therefore has a great potential for designing devices in future. The combination of GPS, GSM and RF on the Repeater shows lots of opportunities for new products.

All electronic devices applied onto Sensor and Repeater hardware have been tested thoroughly. But still some work has to be done. To enable the functionality of calving and heat detection, an algorithm has to be developed combing accelerometer and temperature data. For the design of a sophisticated algorithm, lots of reference data has to be gathered, analyzed and evaluated. At the repeater, a complete error handling for GSM and GPS communication has to be developed and integrated. Finally, the integration of the newly developed system into the smaXtec Monitoring Solution has to be completed. This requires software updates on the smaXtec Base Station and a redesign of the storage database to be able to handle the new types of sensor devices and values.

The systems shows a great potential of assisting stockmen in their daily work. The reproduction cycle of cattle can be optimized and fatality of animals can be avoided, which leads to an increase in economical efficiency for the stock farmer.

List of Abbreviations

ADC	Analog to Digital Converter
A-GPS	Assisted Global Positioning System
APN	Access Point Name
ASCII	American Standard Code for Information Interchange
CPU	Central Processing Unit
DDC	Display Data Channel
EEPROM	Electrically Erasable Programmable Read-Only Memory
ESD	Electrostatic Discharge
FET	Field-Effect Transistor
FIR	Finite Impulse Response
FTP	File Transfer Protocol
GPIO	General Purpose Input/Output
GPRS	General Packet Radio Service
GPS	Global Positioning System
GSM	Global System for Mobile Communications
HTTP	Hypertext Transfer Protocol
IIC or I^2C	Inter-Integrated Circuit
ISR	Interrupt Service Routine
IO	Input Output
JTAG	Joint Test Action Group
LDO	Low Drop-Out
LNA	Low-Noise Amplifier
LSB	Least Significant Bit
MOSFET	Metal-Oxide-Semiconductor Field-Effect Transistor
OPA	Operational Amplifier

PCB	Printed Circuit Board
PHP	PHP: Hypertext Preprocessor
PLF	Precision Livestock Farming
RAM	Random Access Memory
RF	Radio Frequency
RSSI	Received Signal Strength Indication
RTC	Real Time Clock
SAW	Surface Acoustic Wave
SIM	Subscriber Identity Module
SMD	Surface Mounted Device
SMS	Short Message Service
SPI	Serial Peripheral Interface
TI	Texas Instrument
UART	Universal Asynchronous Receiver Transmitter
USCI	Universal Serial Communication Interface
UTC	Universal Time Coordinated

Bibliography

[1] A.R. Frost, C.P. Schofield, S.A. Beaulah, T.T. Mottram, J.A. Lines, and C.M. Wathes. A review of livestock monitoring and the need for integrated systems. *Computers and Electronics in Agriculture*, 14(2):139–159, 1997.

[2] Baniel Berckmans. Automatic on-line monitoring of animals by precision livestock farming. *International Society for Animal Hygiene - Saint-Malo*, pages 27–30, 2004.

[3] K H Kwong, H Goh, C Michie, I Andonovic, B Stephen, T Mottram, and D Ross. Wireless sensor networks for beef and dairy herd management. *Annual International Meeting of the American Association of Agriculture and Biological Engineers*, Providence, Rhode Island, June 29 - July 2 2008. Providence, Rhode Island.

[4] D.J. Patterson, R.A. Bellows, P.J. Burfening, and J.B. Carr. Occurrence of neonatal and postnatal mortality in range beef cattle. i. calf loss incidence from birth to weaning, backward and breech presentations and effects of calf loss on subsequent pregnancy rate of dams. *Theriogenology*, 28(5):557–571, 1987.

[5] Britt Berglund, Jan Philipsson, and Öje Danell. External signs of preparation for calving and course of parturition in swedish dairy cattle breeds. *Animal Reproduction Science*, 15(1):61–79, November 1987.

[6] P.L. Senger. The estrus detection problem: New concepts, technologies, and possibilities. *Journal of Dairy Science*, 77(9):2745–2753, September 1994.

[7] M. Aoki, K. Kimura, and O. Suzuki. Predicting time of parturition from changing vaginal temperature measured by data-logging apparatus in beef cows with twin fetuses. *Animal Reproduction Science*, 86:1–12, March 2005.

[8] Fuller W. Bazer and Neal L. First. Pregnancy and parturition. *J ANIM SCI*, 57:425–460, July 1983.

[9] M. A. Lammoglia, R. A. Bellows, R. E. Short, S. E. Bellows, E. G. Bighorn, J. S. Stevenson, and R. D. Randel. Body temperature and endocrine interactions before and after calving in beef cows. *Journal of Animal Science*, 75(9):2526–2534, 1997.

[10] Dr. Jane A. Parish, Jamie E. Larson, and Dr. Rhonda C. Vann. The estrous cycle of cattle. *Publication P2616*, 2010.

[11] Dr. Jane A. Parish, Dr. Jamie E. Larson, and Dr. Rhonda C. Vann. Estrus (heat) detection in cattle. *Publication P2610*, 2010. Mississippi State University Extension Service.

[12] Sylvia Göllnitz. *Untersuchung von Beziehungen zwischen Indikatoren der Energiebilanz und dem Wiederbeginn der zyklischen Ovarfunktion bei Hochleistungskühen post partum.* PhD thesis, Freie Universität Berlin, 2007.

[13] Simone Odau. *Untersuchungen zur Regulation der Prostagglandinsynthese im bovinen Ovidukt.* PhD thesis, Freie Universität Berlin, 2006.

[14] Jodie A. Pennington. Heat detection in dairy cattle - fsa-4004, 2009.

[15] Glenn Selk. Ansi-4154 heat detection aids for dairy and beef a.i., May 2007. Oklahoma Cooperative Extension Service.

[16] T.R. Wrenn, Joel Bitman, and J.F. Sykes. Body temperature variations in dairy cattle during the estrous cycle and pregnancy. *Journal of Dairy Science*, 41(8):1071–1076, 1958.

[17] K. D. Redden, A. D. Kennedy, J. R. Ingalls, and T.L. Gilson. Detection of estrus by radiotelemetric monitoring of vaginal and ear skin temperature and pedometer measurements of activity. *Journal of Dairy Science*, 76(3):713–721, 1993.

[18] Giuseppe Piccione, Giovanni Caola, and Roberto Refinetti. Daily and estrous rhythmicity of body temperature in domestic cattle. *BMC Physiology*, 3(1):7, 2003.

[19] J.F. Hurnik, G.J. King, and H.A. Robertson. Estrous and related behaviour in postpartum holstein cows. *Applied Animal Ethology*, 2(1):55–68, 1975.

[20] Charles A. Kiddy. Variation in physical activity as an indication of estrus in dairy cows. *Journal of Dairy Science*, 60(2):235–243, 1977.

[21] SR Pecsok, ML McGilliard, and RL Nebel. Conception rates. 1. derivation and estimates for effects of estrus detection on cow profitability. *Journal of Dairy Science*, 77:3008–15, October 1994.

[22] R.J. Esslemont. Economic and husbandry aspects of the manifestation and detection of oestrus in cows. part i - economic aspects. *ADAS Quarterly Review*, 12:175–184, 1974.

[23] J.H. Van Vliet and F.J.C.M. Van Eerdenburg. Sexual activities and oestrus detection in lactating holstein cows. *Applied Animal Behaviour Science*, 50(1):57–69, October 1996.

[24] M. J. Cooper-Prado, N. M. Long, E. C. Wright, C. L. Goad, and R. P. Wettemann. Relationship of ruminal temperature with parturition and estrus of beef cows. *Journal of Animal Science*, 89:1020–27, 2011.

[25] Suzan R. Mathew. Changes in rumen temperature, vaginal temperature and drinking behaviour throughout the estrous cycle in tie-stalled dairy cattle. Master's thesis, The University of Manitoba, 2000.

[26] N. Williamson, J. Alawneh, D. Bailey, and K. Butler. Electronic heat detection. *http://www.side.org.nz/IM_Custom/ContentStore/Assets/7/62/f36fd1a8b6f665-c2652d620643ade3fd/Electronic%20heat%20detection.pdf*, 2006.

[27] S. Kohler, C. Brielmann, K. Hug, and O. Biberstein. Die brunst des rindes automatisch erkennen. *Agrarforschung Schweiz*, 11+12:438–441, 2010.

[28] Israel Martin-Escalona, Francisco Barcelo-Arroyo, and Andrés de la Fuente. On the availability of gnss and terrestrial location techniques: a field study. Technical report, Departamento de Ingeniería Telemática, Universidad Politécnica de Cataluña, 2008.

[29] Tomislav Kos, Mislav Grgic, and Gordan Sisul. Mobile user positioning in gsm/umts cellular networks. In *48th International Symposium ELMAR*, pages 185–188, June 2006.

[30] u-blox AG. *AssistNow u-blox A-GPS services*, April 2011.

[31] Siri Johnsrud and Trajei Aaberge. *DN505: RSSI Interpretation and Timing*. Texas Instruments, 2010.

[32] Elvedin Dizdarevic. Entwicklung einer mehr-antennen-empfangseinrichtung für ein kontaktloses, veterinärmedizinisches sensorsystem. Master's thesis, Institut für Elektronik Technische Universität Graz, 2010.

[33] Texas Instruments. *CC430F513x: MSP430™SoC with RF Core*, November 2010.

[34] Texas Instruments. *TPS6303x: HIGH EFFICIENCY SINGLE INDUCTOR BUCK-BOOST CONVERTER WITH 1-A SWITCHES*, March 2009.

[35] Freescale Semiconductor. *MMA8452Q: 3-Axis, 12-bit/8-bit Digital Accelerometer*, October 2010.

[36] Texas Instruments. *REF33xx: 3.9µA, SC70-3, 30ppm/°C Drift Voltage Reference*, September 2007.

[37] Texas Instruments. *ADS1115: Ultra-Small, Low-Power, 16-Bit Analog-to-Digital Converter with Internal Reference*, October 2009.

[38] STMicroelectronics. *M95512-W: 512kBit serial SPI bus EEPROM with high-speed clock*, September 2010.

[39] Maxim Integrated Products. *DS1390: Low-Voltage SPI RTCs with Trickle Charger*, August 2009.

[40] Gerhard Zancolo. Design and implementation of a signal analysis and processing system for a low power sensor system used to monitor physiological data. Master's thesis, Institute of Electronics Graz University of Technology, 2010.

[41] Texas Instruments. *TPS6120x: Low Input Voltage Synchronous Boost Converter with 1.3A Switches*, February 2008.

[42] Texas Instruments. *TPS3801-xx: Ultra-Small Supply Voltage Supervisors*, October 2010.

[43] u-blox AG. *LEON-G100/G200 quad-band GSM/GPRS Data and Voice Modules Data Sheet*, September 2010. GSM.G1-HW-09001-F.

[44] u-blox AG. *NEO-6 u-blox 6 GPS Modules Data Sheet*, August 2010. GPS.G6-HW-09005-B1.

[45] u-blox AG. *LEON-G100/G200 quad-band GSM/GPRS Data and Voice Modules System Integration Manual*, January 2011. GSM.G1-HW-09002-F3.

[46] STMicroelectronics. *USBLC6-2: Very Low Capacitance ESD Protection*, June 2005.

[47] Round Solutions GmbH & Co KG. *Embedded GSM Antenna ANT-GXE477-V4*, 2011. V.1.0.2011.4.

[48] u-blox AG. *LEA-6 / NEO-6 / MAX-6 u-blox 6 GPS Modules Hardware Integration Manual*, March 2011. GPS.G6-HW-09007-C.

[49] u-blox AG. *C16 telematics reference design GPS and GSM solution with integrated SMT antennas and Chip SIM*, October 2010. GPS.G5-CS-09046-B2.

[50] Texas Instruments. *TPS799xx: 200mA, Low Quiescent Current, Ultra-Low Noise, High PSRR Low Dropout Linear Regulator*, August 2010.

[51] Texas Instruments. *TPS797xx: Ultra-Low I_Q, 50mA LDO Linear Regulators with Power Good Output in SC70 Package*, November 2009.

[52] u-blox AG. *2G GSM/GPRS quad-band Data and Voice Modules AT Commands Manual*, November 2010. GSM.G1-SW-09002-E3.

[53] u-blox AG. *u-blox 6 Receiver Description Including Protocol Specification*, April 2011. GPS.G6-SW-10018-A.